Contrails

AFFDL-TR-67-104
PART I

DEMONSTRATION OF A SUPERSONIC BOX METHOD FOR UNSTEADY AERODYNAMICS OF NONPLANAR WINGS

PART I. GENERAL APPLICATIONS

JAMES J. OLSEN

*** Export controls have been removed ***

This document is subject to special export controls and each transmittal to foreign governments or foreign nationals may be made only with prior approval of the Vehicle Dynamics Division (FDD), Air Force Flight Dynamics Laboratory, Wright-Patterson AFB, Ohio.

Changed to U2 5/10/1976

Contrails

FOREWORD

This report was prepared by the Aerospace Dynamics Branch, Vehicle Dynamics Division, Air Force Flight Dynamics Laboratory, Air Force Systems Command, Wright-Patterson Air Force Base, Ohio. The work was conducted under Project No. 1370, "Dynamic Problems in Flight Vehicles", Task No. 137003, "Prediction and Prevention of Aerothermoelastic Instabilities". Mr. James J. Olsen (FDDS) was the Project Engineer.

The report is published in two parts: Part I, "General Applications"; Part II, "Application to AGARD Planforms". The calculations were performed on the IBM 7094 at WPAFB, using a computer program developed by North American Aviation, Inc., and described in FDL-TDR-64-152, Part IV, "Unsteady Aerodynamics for Advanced Configurations". Recently, improvements have been made to this supersonic unsteady aerodynamic method. The improved methods are described in reports FDL-TDR-64-152, Part VI, "A Supersonic Mach Box Method Applied to T-Tails, V-Tails, and Top-Mounted Vertical Tails" and AFFDL-TR-68-30, "Supersonic Unsteady Aerodynamics for Wings With Trailing Edge Control Surfaces and Folded Tips".

The research covered by this report was conducted from March 1967 to 15 April 1967. The report was completed in September 1968.

This report has been reviewed and is approved.

Walter J. Mykytow

WALTER J. MYKYTOW
Assistant for Research and Technology
Vehicle Dynamics Division
Air Force Flight Dynamics Laboratory

Contrails

ABSTRACT

This report is published in two parts: Part I, "General Applications," and Part II, "Application to the AGARD Planforms."

Part I presents and interprets the calculations of the unsteady aerodynamic prediction method known as the "Nonplanar Mach Box" method. It contains examples of data input and output for the associated computer program and explains the program's interpretation of the user's modal data. Also included are summaries of convergence properties, comparison with exact linearized theory, and a brief outline of the calculations for the Advisory Group for Aeronautical Research and Development (AGARD) planforms. A small part of the extensive tables of Part II is included in Part I.

Part II contains a tabulation of the "Nonplanar Mach Box" results for unsteady generalized force coefficients for the planforms, Mach numbers, mode shapes, and frequencies recommended by AGARD. The tabulation uses the AGARD coordinate system and format. Not all the desired cases could be included because of the program's current limitation to supersonic trailing edges (leading edges can be supersonic or subsonic).

The method was found to be fully workable and constitutes a valuable research and design tool. Convergence and accuracy were found to be comparable to steady-state, planar methods. The computer program is available with sample problems from the Air Force Flight Dynamics Laboratory.

Contrails

Contrails

TABLE OF CONTENTS

Contrails

ILLUSTRATIONS

Contrails

ILLUSTRATIONS (CONTD)

Contrails

TABLES

Contrails

TABLES (CONTD)

Contrails

NOMENCLATURE

A_{ij}	coefficient of a polynomial in X and Y
A_t	coefficient of a polynomial in X and Y
a	speed of sound
b	box length
C_R	root chord
C_T	tip chord
C_{F_α}	slope of second pitching moment curve
C_{L_α}	slope of lift curve
C_{M_α}	slope of pitching moment curve
CPS	cycles per second
f	frequency in CPS
f_i	nondimensional mode shape in AGARD notation
i	$\sqrt{-1}$
i,j	summation indices
k	reduced frequency, $\frac{C_R \omega}{V}$
k_s	reduced frequency, $s\omega/V$
M_∞	Mach number
P_L, P_U	pressure on lower, upper surface
P_j	$(P_L - P_U)$ in the j^{th} mode
Q_{ij}	generalized force coefficient
Q^*_{ij}	generalized force coefficient as printed out by the Mach Box Program
Q'_{ij}	real part of generalized force coefficient in AGARD notation
Q''_{ij}	imaginary part of generalized force coefficient in AGARD notation
q	dynamic pressure, $\rho V^2/2$
r,s	summation indices
r,t	powers

Contrails

NOMENCLATURE (CONTD)

R	upper limit on r summation
R_{ij}	ratio of generalized force coefficients Q_{ij} between two successive computer runs
s	semispan
S	wing planform area
V	airspeed
X	dimensional coordinate
x	x = X, dimensional coordinate
x_1	x/b, nondimensional coordinate
x_{ℓ_e}	position of leading edge in AGARD coordinate system
x_{t_e}	position of trailing edge in AGARD coordinate system
X_{cp}	dimensional position of center of pressure
Y	dimensional coordinate
y	βY, transformed dimensional coordinate; also nondimensional spanwise distance in AGARD coordinate system
y_1	y/b, transformed nondimensional coordinate
Z	dimensional coordinate
z	βZ, transformed dimensional coordinate
z_1	z/b, transformed nondimensional coordinate
α	angle of attack, radians
β	$\sqrt{M_\infty^2 - 1}$
$\tilde{\zeta}$	dimensional coordinate
ζ	$\beta\tilde{\zeta}$, transformed dimensional coordinate
ζ_1	ζ/b, transformed nondimensional coordinate
η	dimensional coordinate
η	$\beta\tilde{\eta}$, transformed dimensional coordinate
η_1	η/b, transformed nondimensional coordinate

Contrails

NOMENCLATURE (CONTD)

λ	$\Delta P/2q$, nondimensional pressure in AGARD notation
$\tilde{\xi}$	dimensional coordinate
ξ	$\xi = \tilde{\xi}$, dimensional coordinate
ξ_1	ξ/b, nondimensional coordinate
ρ	air density
ω	frequency, radians/second

Contrails

SECTION I

INTRODUCTION

Moore and Andrew (Reference 1) developed a numerical method of calculating the velocity potentials and generalized forces on symmetrically vibrating, nonplanar wings at supersonic speeds. The method is based on Ashley's source distribution approach to mutual interference effects in linearized supersonic theory (Reference 2). The method has since been extended to quite general arrays of lifting surfaces (Reference 3). The configuration of interest in the initial computer program and in this report, however, is restricted to a lifting surface consisting of three intersecting planes, as in the sketch below. (The planes need not intersect at right angles.)

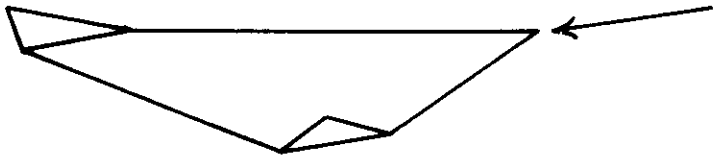

Practical examples of this type of lifting surface are the XB-70 and the F-4 aircraft. The complete theoretical development and some applications of the method are given in Reference 1. However, as is often the case, there was not sufficient time for the authors to fully demonstrate the method to potential users and to elaborate on the intricacies of data handling and interpretation. This report is intended to fulfill that need by serving as a handbook for users of the computer program, by dwelling at length on convergence, correlation, and interpretation of results, and by applying the method to the Advisory Group for Aeronautical Research and Development (AGARD) planforms (Reference 4).

Part I summarizes the initial work which examined the program's interpretation of the user's modal data; presents the convergence effects of Mach number, sweep, frequency, and folded-tip interference; and outlines the application to the standard AGARD planforms. Part II contains an extensive tabulation of generalized force coefficients for the planforms, Mach numbers, frequencies and mode shapes recommended by AGARD. A small sample of the extensive tables of Part II is included in Part I to illustrate the method.

Contrails

SECTION II

INTERPRETATION OF MODE SHAPE INFORMATION

1. COORDINATE SYSTEMS

Moore and Andrew (Reference 1) use three different coordinate systems in developing equations for supersonic unsteady aerodynamics. The coordinate systems, shown in Figure 1, are

1. The physical, dimensional system:

$$\underset{\sim}{X}, \underset{\sim}{Y}, \underset{\sim}{Z}$$
$$\xi, \eta, \zeta$$

2. The transformed, dimensional system:

$$x, y, z$$
$$\xi, \eta, \zeta$$

where

$$x = X$$
$$y = \beta Y$$
$$z = \beta Z$$

3. The transformed, nondimensional system:

$$x_1, y_1, z_1$$
$$\xi_1, \eta_1, \zeta_1$$

where

$$x_1 = x/b$$
$$y_1 = y/b$$
$$z_1 = z/b$$
$$b = \text{box length}$$

In working with a program developed by others, the user is often uncertain about the coordinate system to be used. Questions naturally arise, as they did in Reference 5, such as:

> "Are the deflections and/or coordinates normalized by some typical dimensions? Are the coordinates transformed in any manner from physical, dimensional coordinates?"

A convenient method for answering those questions is contained in the Appendix. The results for this program indicate that the user always works in the physical, dimensional X, Y, Z system. Using equations in the Appendix, the program was applied to rectangular wings in plunge and rotation about the leading edge. Table I gives the input data, and Table II summarizes the generalized force coefficients obtained. The results show that each of the

Contrails

powers r and t (defined in the Appendix) must be zero and that all transformations of coordinates are purely internal features of the program, indicating that the user need only work in his original dimensional coordinate system.

2. MODE SHAPES

The modal deflection patterns can be given to the program in either of two ways:

1. Polynomial coefficients
2. Deflections Z at discrete X, Y locations

The program is set up to use the polynomial coefficients directly to evaluate downwash and generalized forces. If the data are given as discrete deflections, then the program fits a least squared error polynomial surface to the deflection data and proceeds from there with the coefficients of the polynomial.

Reference 1 gives the initial or fitted polynomials in an unusual format. The coefficients A_t define the polynomial surface.

$$Z(X,Y) = \sum_{r=0}^{R} \sum_{s=0}^{r} A_t \, X^{r-s} \, Y^{s}$$

where

$$t = r\left(\frac{r+1}{2}\right) + (s+1)$$

Application of these formulas can be seen in the following example:

$$\begin{aligned} Z = {} & A_1 \\ & + A_2 X + A_3 Y \\ & + A_4 X^2 + A_5 XY + A_6 Y^2 \\ & + A_7 X^3 + A_8 X^2 Y + A_9 X Y^2 + A_{10} Y^3 \\ & + \cdots \end{aligned}$$

Hence if the user desires a mode to be a quadratic in the spanwise variable Y he must specify all coefficients through A_6. Further, all mode shapes are treated as symmetric about the wing center line.

3. GENERALIZED FORCES

Reference 1 defines the generalized force coefficient Q_{ij} as:

$$Q_{ij} = \frac{1}{qS} \iint_S Z_i(X,Y) \, \Delta P_j(X,Y) \, dX \, dY$$

Contrails

where

$Z_i(X,Y)$ = deflection in i^{th} mode

$\Delta P_j(X,Y)$ = pressure differential in j^{th} mode

Using a plunge mode given by $Z_1 = A_1$ and a rotation about the leading edge given by $Z_2 = A_2X$ the generalized force coefficients become

$$Q_{11} = -ikA_1^2 C_{L_\alpha}/C_R$$

$$Q_{21} = -ikA_1 A_2 C_{M_\alpha}$$

$$Q_{12} = -A_1 A_2 (C_{L_\alpha} + ikC_{M_\alpha})$$

$$Q_{22} = -A_2^2 C_R (C_{M_\alpha} + ikC_{F_\alpha})$$

Examination of the output in Table II, however, reveals that the computer program interprets the generalized force coefficients to be just the transpose of the coefficient format given in Reference 1. Therefore

$$Q_{ij} = \frac{1}{qS} \iint_S \Delta P_i(X,Y)\, Z_j(X,Y)\, dXdY$$

Contrails

SECTION III

CONVERGENCE

The convergence of the nonplanar Mach box method should depend, as it does for the planar method, on Mach number, sweep, and frequency. The added complication of the provision for more general planforms also should be important. There is an enormous number of variations which could be made to check convergence; however, this Section is limited to three basic investigations:

1. An investigation of the effects of Mach number and sweep at zero frequency;

2. An investigation of the effects of frequency and mode shape on a delta wing at a low supersonic Mach number;

3. An investigation of the effects of tip fold angle on a delta wing at a low supersonic Mach number and high frequency.

1. MACH NUMBER AND SWEEP EFFECTS

Figure 2 shows rectangular and delta wings with superimposed Mach lines corresponding to Mach numbers 1.5 and 3.0. Although the program generally allows up to 20 chordwise boxes, these planforms have an upper chordwise limit of 15 at $M_\infty = 3.0$ because at that point the maximum number of 30 spanwise boxes is reached. These particular planforms and Mach numbers were chosen to also provide a subsonic and supersonic leading edge on the delta and to move the tip Mach lines across the center of the trailing edge of the rectangle. The modes used were zero frequency plunge and pitch to yield generalized force coefficients directly related to C_{L_α} and C_{M_α}. Recall that in Section I, it was shown that the computer program utilizes the generalized force coefficient

$$Q_{ij} = \frac{1}{qS} \iint_S (P_L - P_U)_i \; Z_j \; dX \, dY$$

Then, if we set $Z_1 = A_1$ and $Z_2 = A_2 X$ at zero frequency, we can obtain the generalized force coefficients

$$Q_{21} = - A_1 A_2 C_{L_\alpha}$$

$$Q_{22} = - A_2^2 C_R C_{L_\alpha}$$

If we set $A_1 = -\sqrt{C_R}$ and $A_2 = 1/\sqrt{C_R}$, we can obtain

$$Q_{21} = C_{L_\alpha}$$

$$Q_{22} = -C_{M_\alpha}$$

Tables III and IV illustrate the data input for the rectangular and delta wings. The results are shown in Figures 3, 4, and 5.

Contrails

Figure 3 is a plot of C_{L_α} versus the number of boxes used along the root chord. The circles represent predictions of the Mach box method. The lines represent the exact results of linearized theory (of which the Mach box scheme is a munerical approximation). The data near the bottom of the graph are for the rectangular wing at Mach 3.0. The convergence and accuracy are both excellent which, of course, is expected since this is about the most favorable case imaginable. The data second from the bottom are for the delta wing at Mach 3.0. Again the convergence and accuracy are excellent. The data third from the bottom represent the rectangle at Mach 1.5. Convergence is somewhat slower than the earlier cases and the Mach box prediction for C_{L_α} persists at a value slightly higher than the exact value. Finally, the top set of data are for the delta wing at Mach 1.5. Here the convergence and accuracy have deteriorated. It is interesting to note that in the last case, consideration of convergence in the three groups

a. 5, 9, 13, 17

b. 6, 10, 14, 18

c. 7, 11, 15, 19 boxes

shows rather smooth variation with the last group enjoying the best convergence and accuracy.

Figure 4 compares the Mach box and exact linearized predictions for center of pressure. The lower graph is for the rectangular and delta wings at Mach 3.0. For both cases accuracy and convergence are excellent. The upper graph is for the delta and rectangular wings at Mach 1.5 Convergence and accuracy are excellent for the rectangular wing. Convergence for the delta wing is only fair, but overall accuracy is good.

Consideration of the data of Figures 3 and 4 reveals that the lift is somewhat higher than desired at the low Mach numbers, but that the lift distribution is generally predicted rather well. This aspect is revealed further in Figure 5, a plot of C_{M_α} vs C_{L_α} for the delta wing at Mach 1.5 with varying numbers of chordwise boxes. The solid diagonal line on the figure represents the exact linearized result for delta wings that $C_{M_\alpha} = \frac{2}{3} C_{L_\alpha}$. Therefore any point above and to the left of the solid line represents a slope of C_{M_α} vs C_{L_α} greater than 2/3. The converse applies to points below and to the right. The + at $C_{L_\alpha} = 3.04$ represents the exact linearized prediction for this particular delta. The predictions of the Mach box method are again conveniently classified into three groups:

a. 7, 11, 15, 19 boxes denoted by Δ

b. 5, 9, 13, 17 boxes denoted by o

c. 6, 10, 14, 18 boxes denoted by ∇

For the first group the lift is lower than the exact value, and the center of pressure is forward of the exact value. For the second group the lift is high, but the center of pressure is predicted quite well. For the third group the lift is higher than the exact value, and the center of pressure is aft of the exact value. Each of the three groups of Mach box predictions is approaching the correct lift distribution with increasing number of boxes, even though the magnitude of the lift is slightly in error.

Contrails

This suggests a possible empirical modification to the computer program for later use in unsteady flow with more complicated mode shapes. For a given number of chordwise boxes, one could check the Mach box prediction of C_{L_α} against the exact linearized result for that wing and Mach number. He could then determine what empirical modification to the uniform source strength would bring the two predictions into agreement. Then as other calculations are performed for cases where source strength varies over the wing the empirical correction can be applied to each local source strength in proportion to its initial value.

2. FREQUENCY EFFECTS

The planform used is again the delta wing of Figure 2. The wing is subject to plunge, rotation, parabolic camber and cubic camber modes at a Mach number of 1.5 and at frequencies of 0.0, 4.4445, and 8.889 cps. The four mode shapes can be expressed by polynomials:

$$Z_1 = 5.4772$$

$$Z_2 = 0.18257X$$

$$Z_3 = 0.18257X - 0.006085X^2$$

$$Z_4 = 0.18257X - 0.018257X^2 + 0.004057X^3$$

The four mode shapes are presented in Figure 6. The cubic term in the fourth mode has been made large to emphasize its influence. The data are presented in Table V; the results are summarized in Figures 7 through 10.

Figures 7, 8, and 9 are plots of the absolute value of the lift coefficients in the four modes of Figure 6 versus the number of boxes used along the chord. The results are plotted in terms of the fractional deviation of the lift with N boxes from the lift with 19 boxes, $\frac{Q_{J_1}(N)}{Q_{J_1}(19)} - 1.$

Hence a value of 0.05 on the ordinate would indicate that the lift with N boxes is 5% higher than the lift with 19 boxes.

Figure 7 illustrates the results for zero frequency. For modes 2, 3, and 4 the lift for 6 boxes along the chord is about 11% to 12% higher than the lift for 19 boxes. As the number of boxes is increased the predictions undergo a convergent oscillation, indicating that at the upper limit of the allowable number of boxes, the predictions are probably within 3% of final converged solutions. At zero frequency, there is no lift in mode 1, the plunge mode.

Figure 8 repeats Figure 7 except that the reduced frequency has been increased to k = 0.5. The character of the convergence is nearly identical to that of k = 0.0. In fact, if the reader could superimpose the two Figures, he would find very little difference in modes 2, 3, and 4.

Figure 9 repeats Figures 7 and 8 except that the reduced frequency has been increased to k = 1.0. Here again, the type of convergence is relatively unchanged.

Figures 7, 8, and 9 can lead to two important conclusions:

1. The type of convergence is only slightly affected by the type of mode (plunge, rotation, parabolic camber, cubic camber);

2. The type of convergence is only slightly affected by reduced frequency ($0 \leq k \leq 1$).

Contrails

This would indicate that perhaps the answers could be converged more rapidly by employing the empirical technique of weighting the generalized forces by the factor which causes C_{L_α} to agree with experiment, exact theory, or some converged solution. For instance, for 14 boxes along the chord we have the following results from Figures 7, 8, and 9:

$$Q_{J_1}(14)/Q_{J_1}(19)$$

J	k = 0	k = 0.5	k = 1.0
1	-	1.047	1.046
2	1.046	1.046	1.045
3	1.051	1.049	1.043
4	1.049	1.049	1.050

The result for J = 2, k = 0 corresponds to C_{L_α}. Therefore, we divide all the other answers by 1.046 and obtain:

$$\frac{Q_{J_1}(14)/Q_{J_1}(19)}{C_{L_\alpha}(14)/C_{L_\alpha}(19)}$$

J	k = 0	k = 0.5	k = 1.0
1	-	1.001	1.0
2	1.0	1.0	0.9990
3	1.005	1.003	0.9971
4	1.003	1.003	1.004

The results are plotted in Figure 10 for varying numbers of boxes along the root chord. The results indicate that the convergence process could be rapidly accelerated by continually weighting the generalized forces by a factor which would cause the static C_{L_α} to assume the "correct" value. Figure 10 reveals that the total "error" for some oscillating mode with considerable camber is only 1% or 2% different that the "error" in C_{L_α} and that this tendency is relatively insensitive to frequency for k's up to at least 1.0.

3. INTERFERENCE EFFECTS

The final aspect of convergence that is examined is the provision of the program to handle wings with folding tips. The delta wing of Figure 2 is studied at Mach 1.5, a frequency of 8.889 cps (k = 1), and in a cubic camber mode. The wing is folded at various angles about a line midway between the root and the tip. The lift in the camber mode is examined for increasing numbers of boxes. In order to evaluate lift, the first mode must be a "dummy" plunge mode while the second is the camber mode. The input data are shown in Table VI; the results are shown in Figure 11. The results indicate that the convergence of the absolute value of the lift in the camber mode improves as the tip fold angle is progressively increased from 0° to 90°. The 3% deviation at a fold angle of 0° is decreased to a deviation of less than 1% for 90° fold.

Contrails

SECTION IV

APPLICATION TO THE AGARD PLANFORMS

At the 20th meeting of the AGARD Panel on Structures and Materials, the NATO countries were invited to perform unsteady aerodynamic calculations on a set of standard planforms. The coordinate system and the definition of generalized forces to be used differ from those used in this report so that some interpretation is necessary. Further, the program is currently capable only of analyzing symmetric vibration modes, so that duplication of the AGARD antisymmetric modes is not possible. Part II of this report contains the detailed tabulated results of the application of this program.

The standard AGARD format requires the use of a nondimensional coordinate system which is denoted by x, y, z. The origin of coordinates is at the center of the root chord, and all coordinates are made nondimensional by dividing by the semispan s. The Mach box program uses a dimensional coordinate system, originating at the apex.

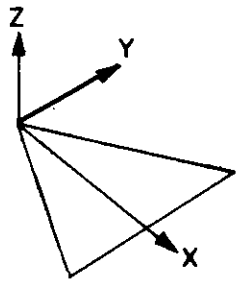

Mach Box

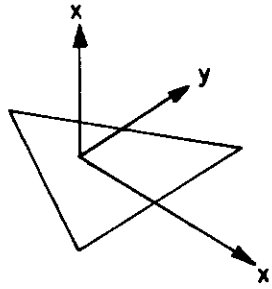

AGARD

Hence we have the transformations

$$y = Y/s \qquad z = Z/s \qquad x = (X - \frac{C_R}{2})/s$$

The AGARD definition of a generalized force coefficient is

$$Q_{ij} = -\int_{y=-1}^{+1}\int_{x=x_{l_e}}^{x_{t_e}} f_i(x,y)\,\lambda_j(x,y)\,dx\,dy$$

where

$$\lambda_j(x,y) = \Delta P_j(x,y)/2q$$

$$f_i(x,y) = Z_i(x,y)/s$$

Then in the Mach box notation we have

$$Q_{ij} = -\int_{y=-1}^{+1}\int_{x=x_{l_e}}^{x_{t_e}} \frac{Z_i(x,y)}{s}\,\frac{\Delta P_j(x,y)}{2q}\,dx\,dy$$

Contrails

Returning to the dimensional X, Y, Z coordinate system

$$Q_{ij} = \frac{-1}{2qs^3} \int_{Y=-s}^{+s} \int_{X=X_{\ell_e}}^{X_{t_e}} Z_i(X,Y)\, \Delta P_j(X,Y)\, dX\, dY$$

In terms of the Mach box program definition (call it Q^*_{ij})

$$Q_{ij} = \frac{-1}{2qs^3} (Q^*_{ij})^T \quad qS = -(Q^*_{ij})^T \frac{(C_R + C_T)}{2s^2}$$

where the superscript "T" denotes "transpose" and we have taken the area definition of any trapezoidal wing $S = (C_R + C_T)s$. Then for a given set of mode shapes, to put the data in the AGARD format we must (1) change the sign and transpose Q_{ij}, and (2) multiply by the average chord and divide by the semispan, squared.

A convenient way to aid the changes automatically is to choose dimensions so that

$$\frac{C_R + C_T}{2s^2} = 1.0$$

This will occasionally necessitate the dimensions to vary from those of AGARD, but since the AGARD generalized force coefficients are nondimensional, they should be unaffected.

A final note in this regard is that the reduced frequency is defined as $k_s = s\omega/v$ in the AGARD format and that the generalized force coefficients are broken into real and imaginary parts:

$$Q_{ij} = Q'_{ij} + ik_s Q''_{ij}$$

1. THE ASPECT RATIO 2.0 RECTANGULAR WING

Figure 12 depicts the aspect ratio 2.0 rectangular wing. Both the root chord and the semispan can be set equal to 1.0 which is the value specified by AGARD. The Mach box program can be used at the desired Mach numbers of 1.05, 1.20, and 2.00. Figure 13 shows the Mach box program's approximation of the wing and diaphragm areas for the three Mach numbers used in these calculations. The necessary oscillatory frequencies to yield the desired values of k can be obtained from

$$k_s = \frac{s\omega}{V} = \frac{2\pi s f}{M_\infty a}$$

Hence for a = 1000 ft/sec and s = 1 ft, we have

$$f_{cps} = 159.16 (M_\infty k_s)$$

Contrails

Table VII illustrates the frequencies required at each Mach number and reduced frequency. Table VIII gives the mode shapes in the AGARD and Mach box coordinate systems. Table IX summarizes the real part of the generalized force for $k_s = 0.0$. Because of their rather specialized interest, the complete tables for $k_s \neq 0$ are not reproduced here but are available in Part II of this report.

2. THE ASPECT RATIO 1.45 TAPERED, SWEPT-BACK WING

Figure 14 depicts the aspect ratio 1.45 tapered, swept-back wing. We find that interpretation of the Mach box output in terms of the AGARD requirements are facilitated if we change the semispan from 1.0 to 1.379. Therefore

$$s = 1.379$$

$$C_R = 2.224$$

$$C_T = 1.579$$

Then $\frac{C_R + C_T}{2s^2} = 1.0$ and the AGARD generalized force matrix can again be obtained from the Mach box output by a simple change of sign and transposition. The desired Mach numbers are 2.0, 1.2, and 1.04; however, to obtain a supersonic trailing edge the minimum Mach number must be 1.057. Figure 15 shows the Mach box program's approximation of the wing and diaphragm areas for the three Mach numbers used. The desired values of reduced frequency are 0, 0.5, and 1.4. The necessary oscillatory frequencies required to obtain the desired values of k_s can be obtained from

$$f = \frac{M_\infty a k_s}{2\pi s}$$

Since $s = 1.379$ and $a = 1000.0$, $f = 115.4\ (M_\infty k_s)$.

Table X illustrates the frequencies required at each Mach number and reduced frequency while Table XI gives the mode shapes in the AGARD and Mach box coordinate systems. Table XII contains zero frequency results for the AGARD generalized force coefficient Q'_{ij}.

3. THE ASPECT RATIO 4.0 ARROWHEAD WING

Figure 16 depicts the AGARD aspect ratio 4.0 arrowhead wing. The root chord has the same length as the semispan and the tip chord is zero. Therefore to force $\frac{C_R + C_T}{2s^2} = 1.0$, we must change s from the AGARD value of 1.0 to 0.5. The Mach box program can be run at the desired Mach numbers of 2.0, 1.5621, and 1.25. However, at the desired Mach number of 1.1 the trailing edge is subsonic, therefore the current Mach box program must be run at a minimum Mach number of 1.12 to insure a supersonic trailing edge. Figure 17 shows the Mach box program's approximation of the wing and diaphragm areas at the four Mach numbers used. The oscillatory frequencies necessary to yield the desired values of k_s can be obtained from

$$f_{cps} = \frac{M_\infty a k_s}{2\pi s} = 318.3\ (M_\infty k_s)$$

Table XIII gives the frequencies required at each Mach number and reduced frequency. Table XIV gives the mode shapes in the AGARD and Mach box coordinate systems. Table XV gives Q'_{ij} for $k_s = 0.0$.

Contrails

SECTION V

CONCLUSIONS AND RECOMMENDATIONS

1. CONCLUSIONS

a. The user of the folded tip Mach box computer program need only work in a physical, dimensional, right-hand coordinate system X, Y, Z.

b. When the symmetric mode shapes are given by polynomial coefficients the definition of coefficients is (where Y should be interpreted as $|Y|$)

$$Z(X,Y) = A_1 + A_2X + A_3Y + A_4X^2 + A_5XY + A_6Y^2 + A_7X^3 + A_8X^2Y + A_9XY^2 + A_{10}Y^3 + \cdots$$

c. The generalized force coefficients are defined as

$$Q_{ij} = \frac{1}{qS} \iint_S (P_L - P_U)_i \, Z_j \, dX \, dY$$

d. For rectangular and delta wings at $M_\infty = 3.0$, convergence and accuracy of lift and center of pressure were excellent. At $M_\infty = 1.5$ convergence was generally slower and accuracy slightly less.

e. The bulk of any error introduced by the Mach box system could be eliminated by correcting all generalized forces in proportion to a C_{L_α} correction.

f. The convergence properties were generally insensitive to frequency for $0 \leq k \leq 1$. The convergence properties were also only slightly influenced by the type of mode treated.

g. For the conditions analyzed, folding the wing tip tended to increase convergence.

h. The AGARD planforms can be treated directly with the Mach box program, with some attention required to coordinate systems, symmetry of mode shapes, and interpretation of results.

i. The Nonplanar Mach Box computer program is now a completely workable, useful research and design tool. The latest version of the program is available from the Air Force Flight Dynamics Laboratory.

2. RECOMMENDATIONS

a. Succeding reports which discuss the development of similar computer programs should be more explicit in their treatment of coordinate systems. Care should be taken in implementing the definitions of generalized force coefficients.

b. Succeeding programs should relate polynomial coefficients for mode shapes directly to the powers of X and Y involved, $Z(X,Y) = \sum_{ij} A_{ij} X^i Y^j$

Contrails

c. Simple C_{L_α} corrections can be included in the program to weight all generalized force coefficients and improve convergence. These corrections could be tabulated from exact linearized theory for simple planforms, or from numerical results with great numbers of boxes for more complicated planforms.

d. The program should be expanded to accommodate antisymmetric as well as symmetric modes.

REFERENCES

1. Moore, M. and Andrew, L., Unsteady Aerodynamics for Advanced Configurations. Part IV, Application of the Supersonic Mach Box Method to Intersecting Planar Surfaces, FDL-TDR-64-152, Part IV, Air Force Flight Dynamics Laboratory, Wright-Patterson Air Force Base, Ohio, May 1965.

2. Ashley, H., Supersonic Airloads on Interfering Lifting Surfaces by Aerodynamic Influence Coefficient Theory, Boeing Report D2-22-67, November 1962.

3. Andrew, L., Unsteady Aerodynamics for Advanced Configurations, Part VI, Application of the Supersonic Mach Box Method to T-Tails, V-Tails, and Top-Mounted Verticals, FDL-TDR-64-152, Part VI, Air Force Flight Dynamics Laboratory, Wright-Patterson Air Force Base, Ohio, 1967.

4. Woodcock, D., Dat, R., Bergh, H., and Lashka, B., Planforms for Calculations of Unsteady Air Forces, Report of working party appointed at 19th AGARD Structures and Materials meeting, May 1965.

5. Olsen, J. J., Demonstration of a Transonic Box Method for Unsteady Aerodynamics of Planar Wings, AFFDL-TR-66-121, Air Force Flight Dynamics Laboratory, Wright-Patterson Air Force Base, Ohio, October 1966.

Contrails

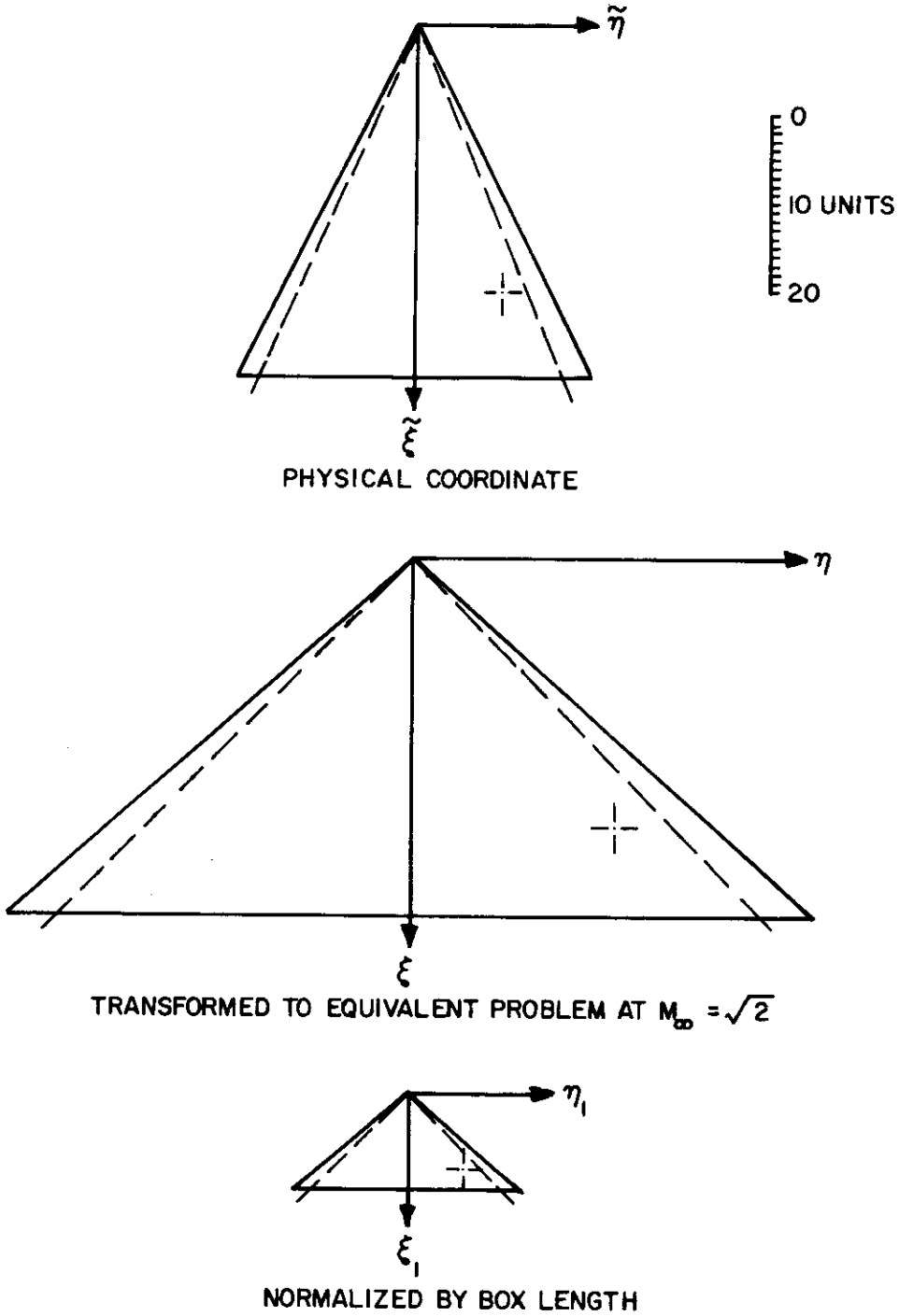

Figure 1. Succession of Coordinate Systems

Contrails

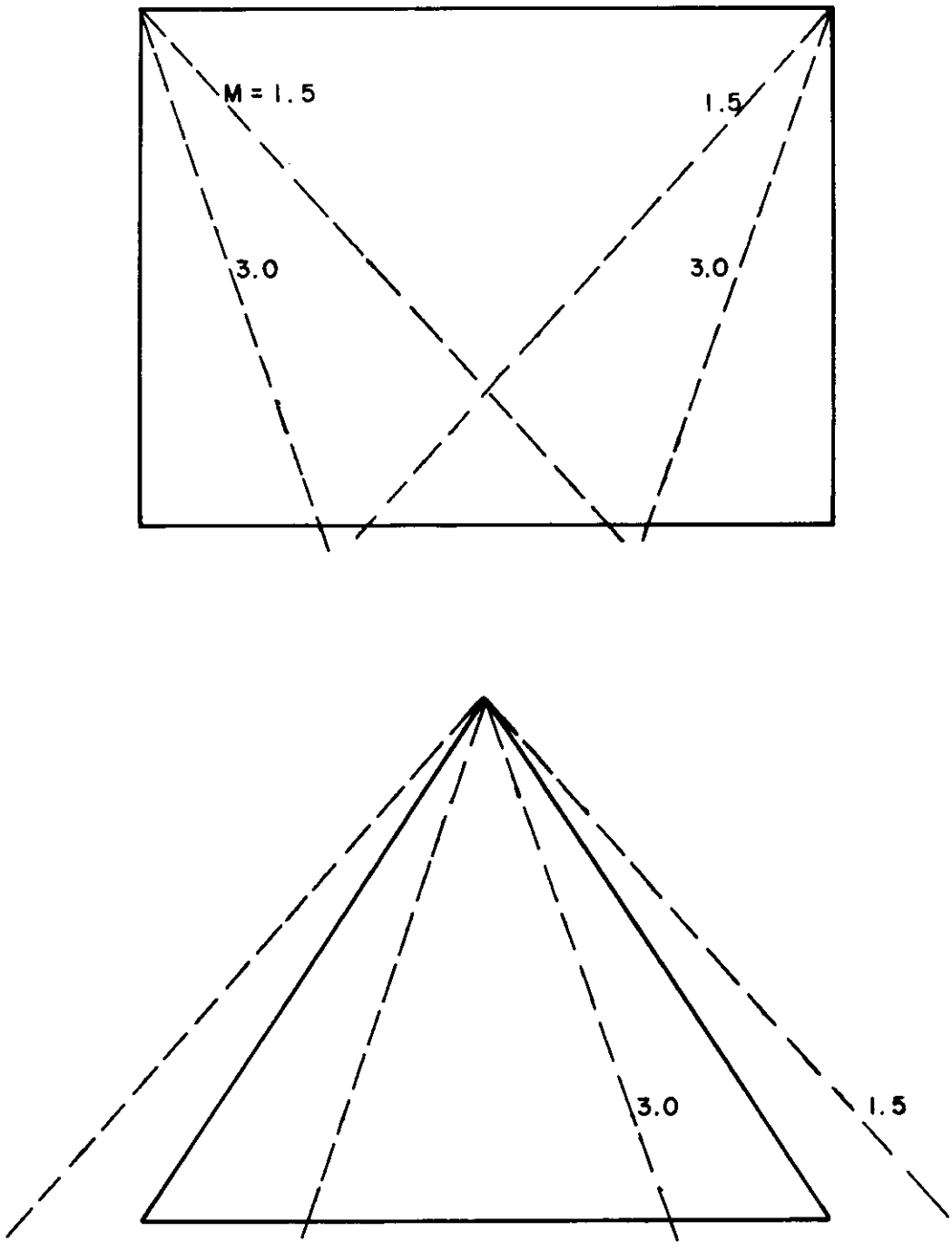

Figure 2. Planforms Used to Evaluate Sweep and Mach Number Effects

Contrails

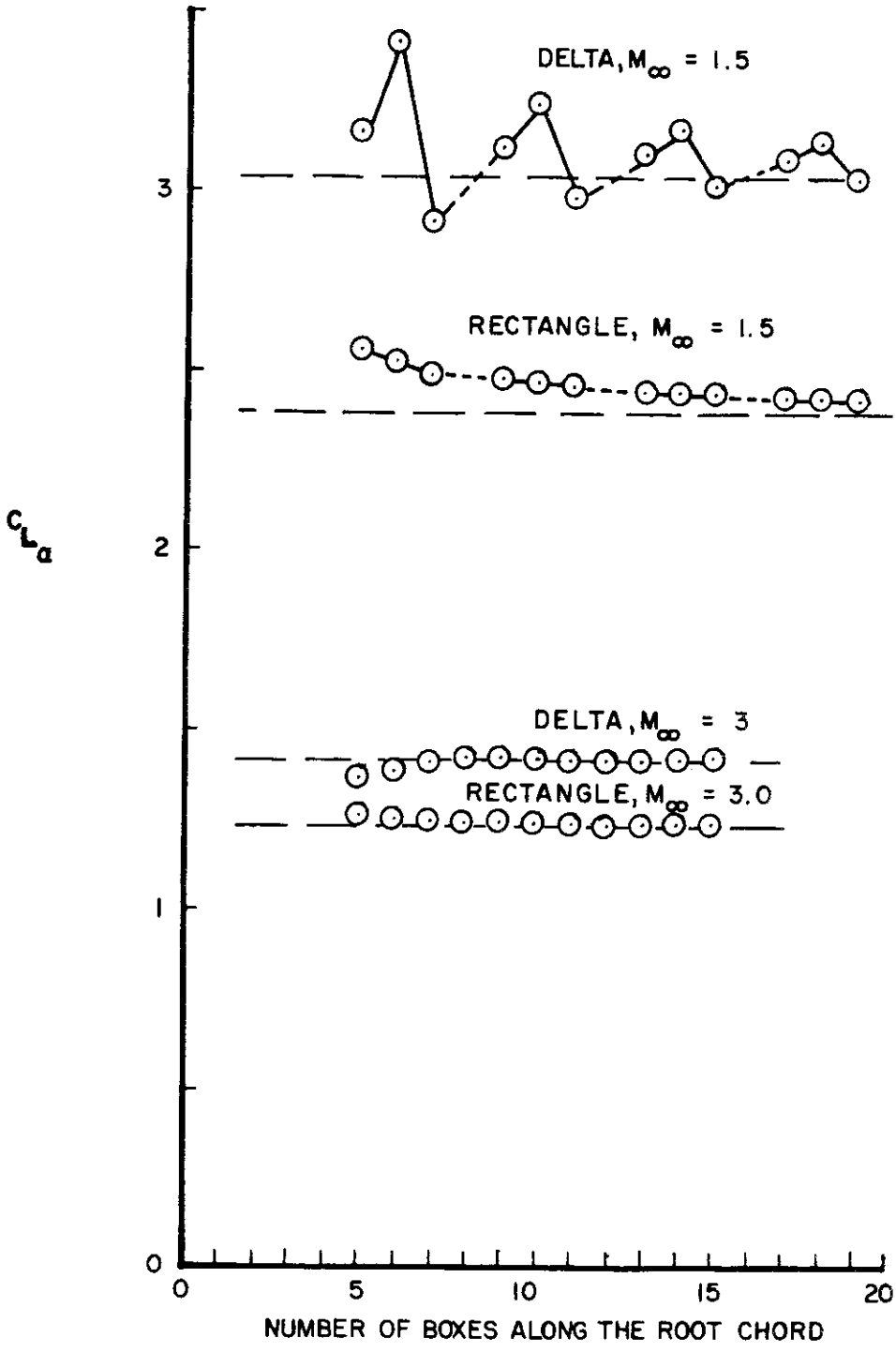

Figure 3. Convergence of C_{L_α} for Rectangular and Delta Wings at M_∞ = 1.5 and 3.0

Contrails

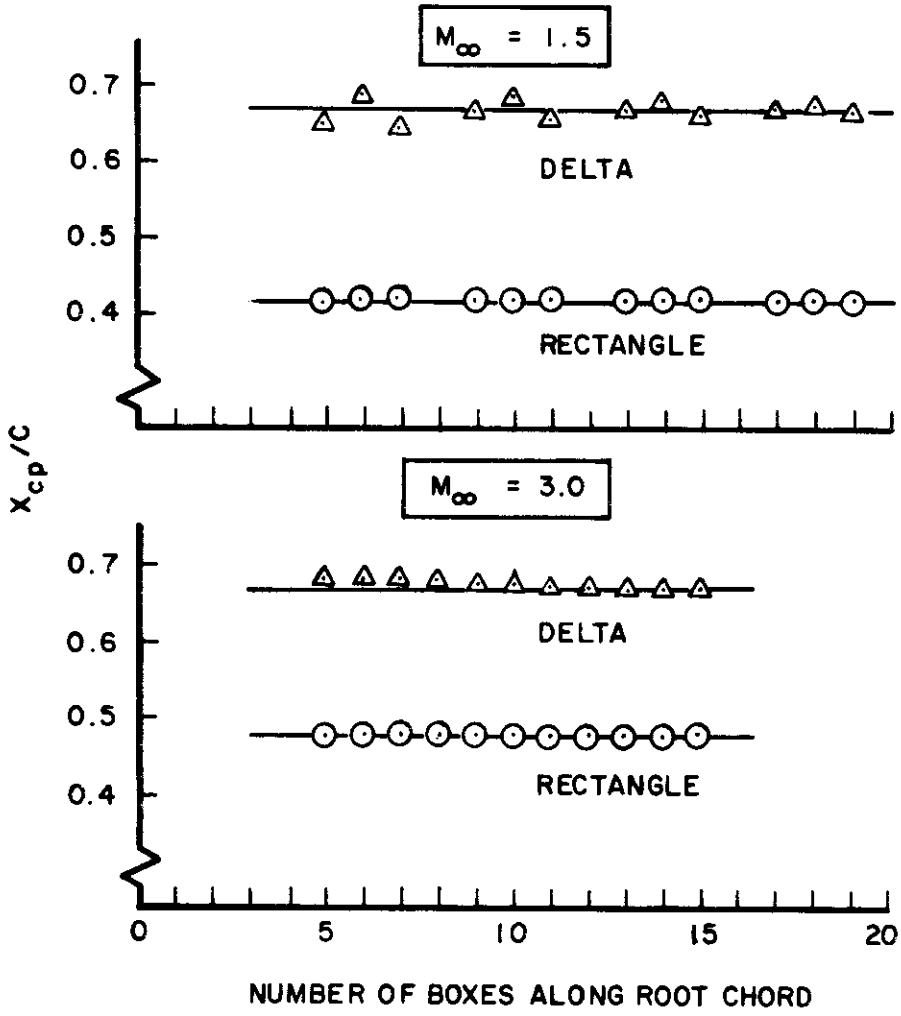

Figure 4. Convergence of Center of Pressure for Rectangular and Delta Wings at M_∞ = 1.5 and 3.0

Contrails

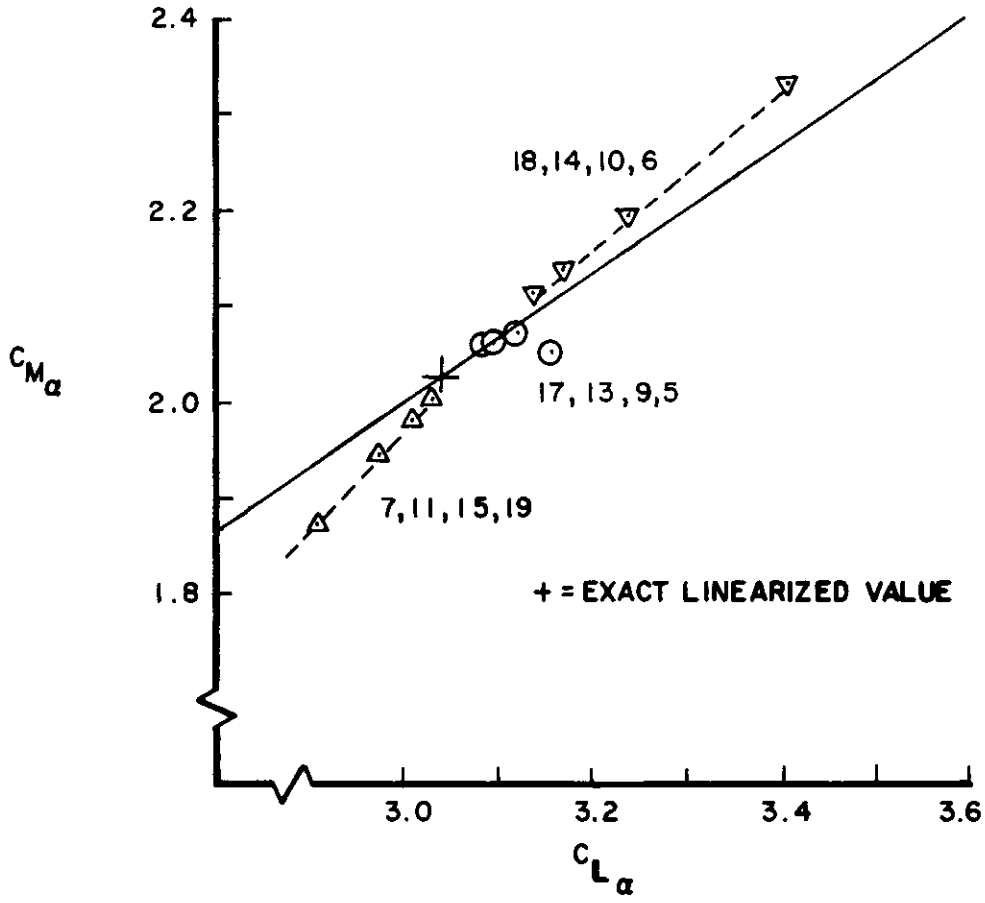

Figure 5. Convergence of C_{M_α} vs C_{L_α} for the Delta Wing at Mach 1.5

Contrails

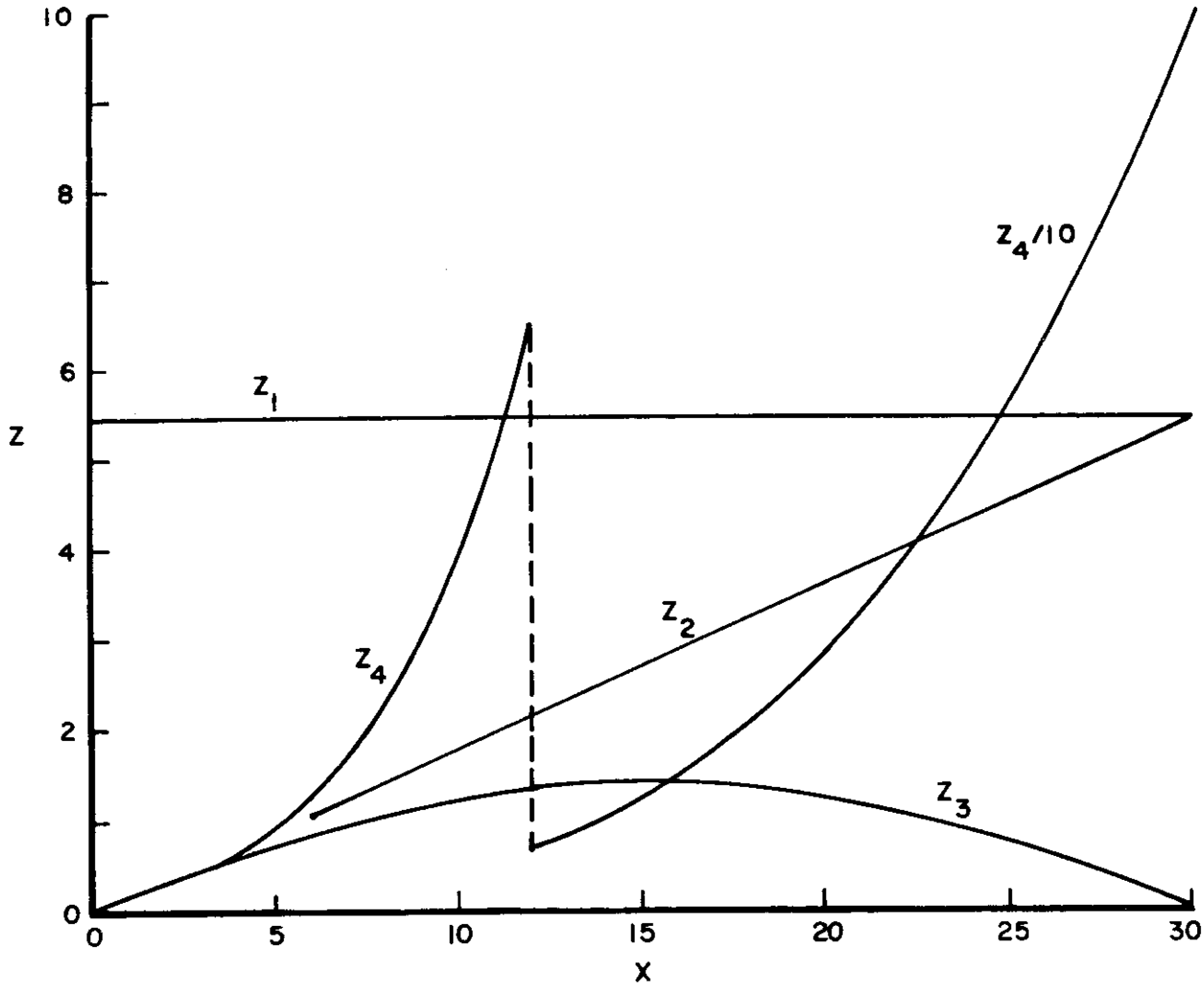

Figure 6. Mode Shapes for the Frequency-Mode Shape Convergence Study

Contrails

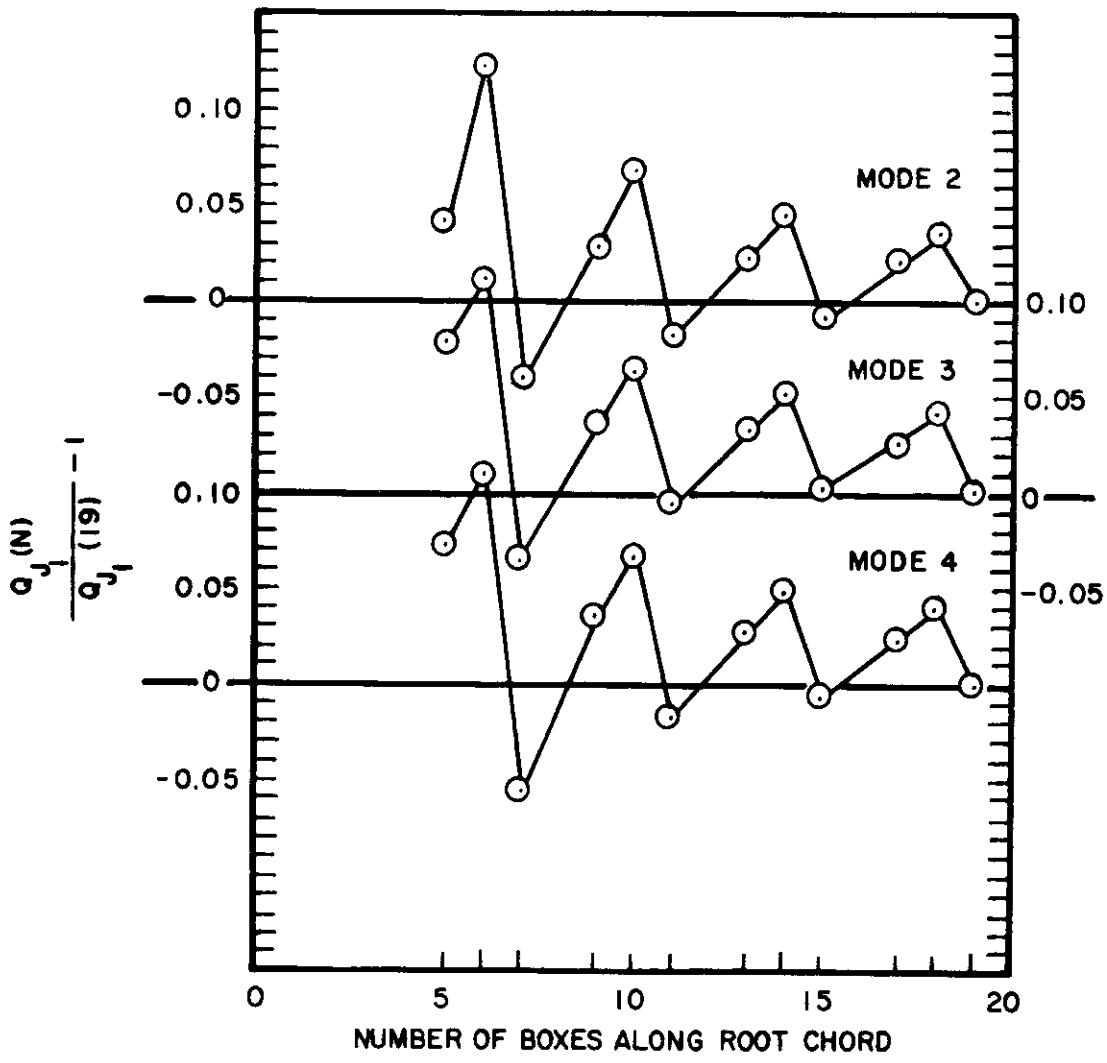

Figure 7. Variation of Lift Coefficient From Its Value for 19 Boxes, k = 0.0

Contrails

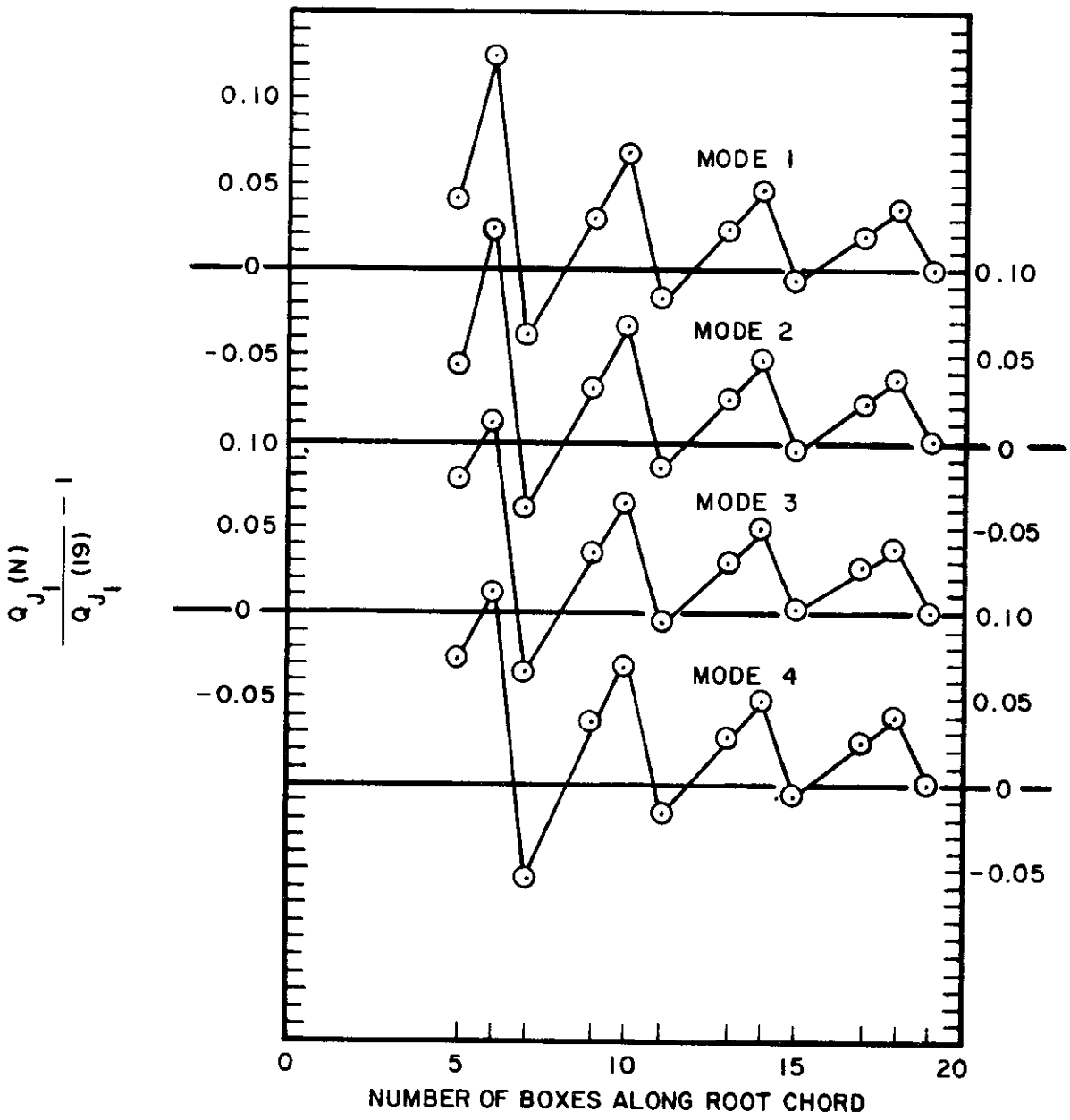

Figure 8. Variation of Oscillatory Lift Coefficient From Its Value for 19 Boxes, k = 0.5

Contrails

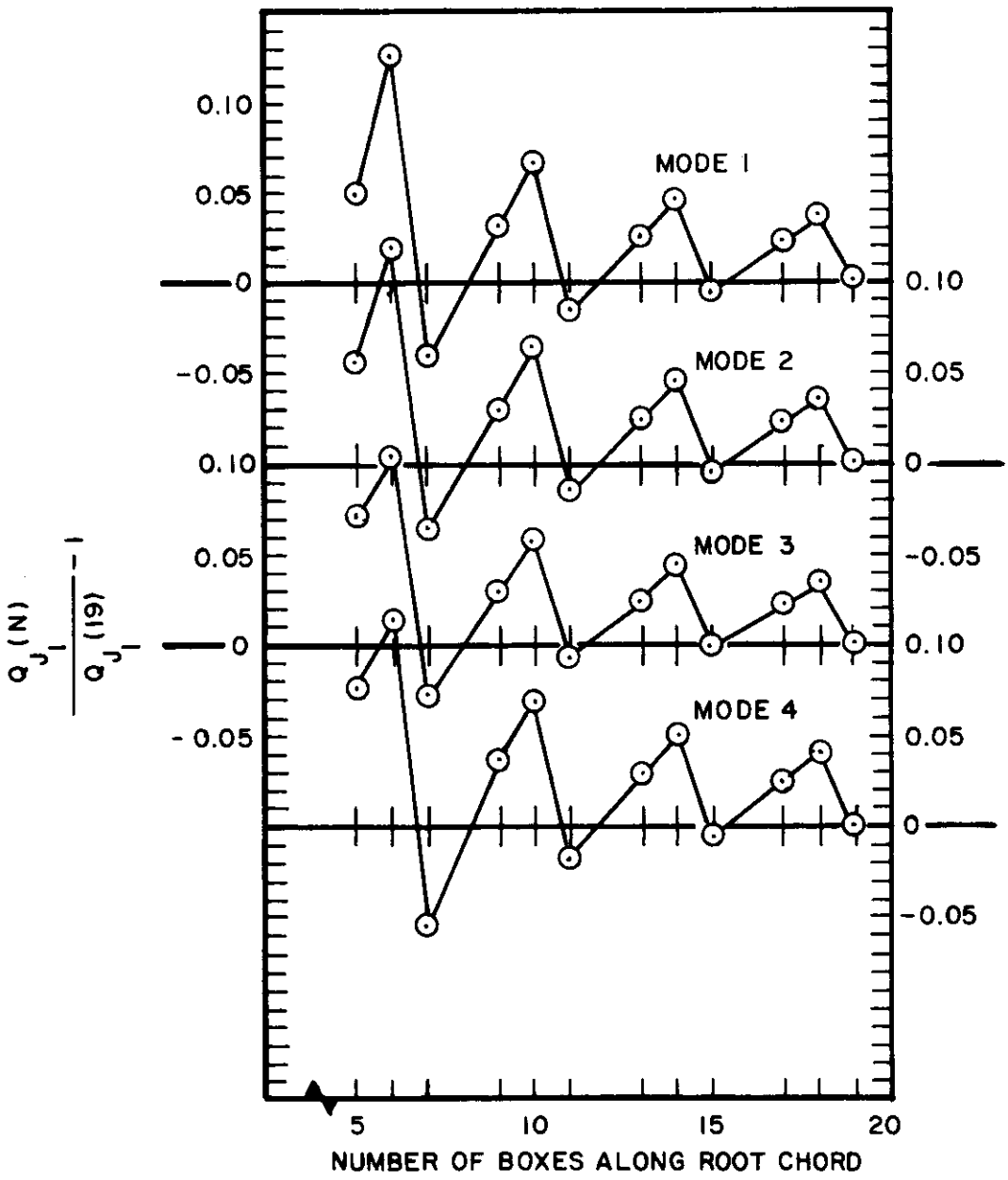

Figure 9. Variation of Oscillatory Lift Coefficient From Its Value for 19 Boxes, k = 1.0

Contrails

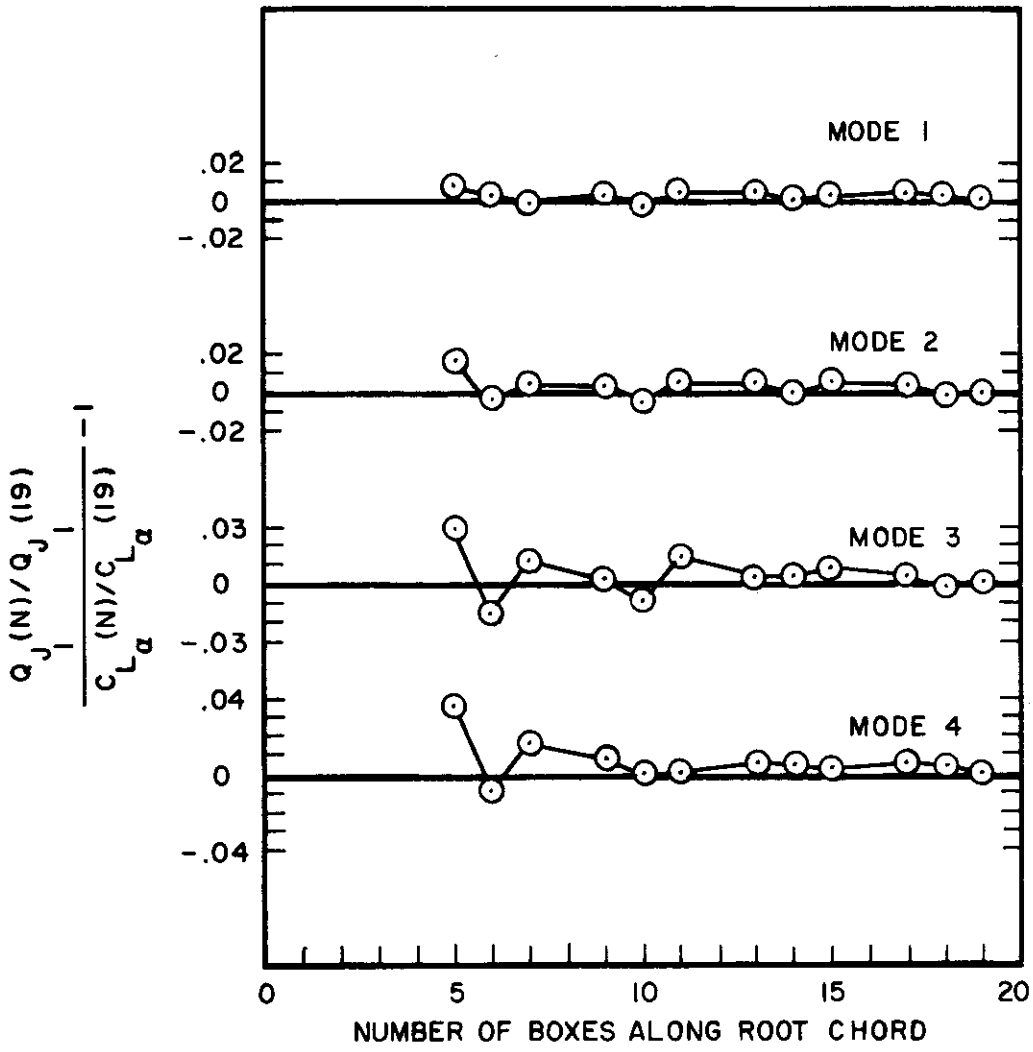

Figure 10. Variation of the Total "Error" From the Steady-State "Error"

Contrails

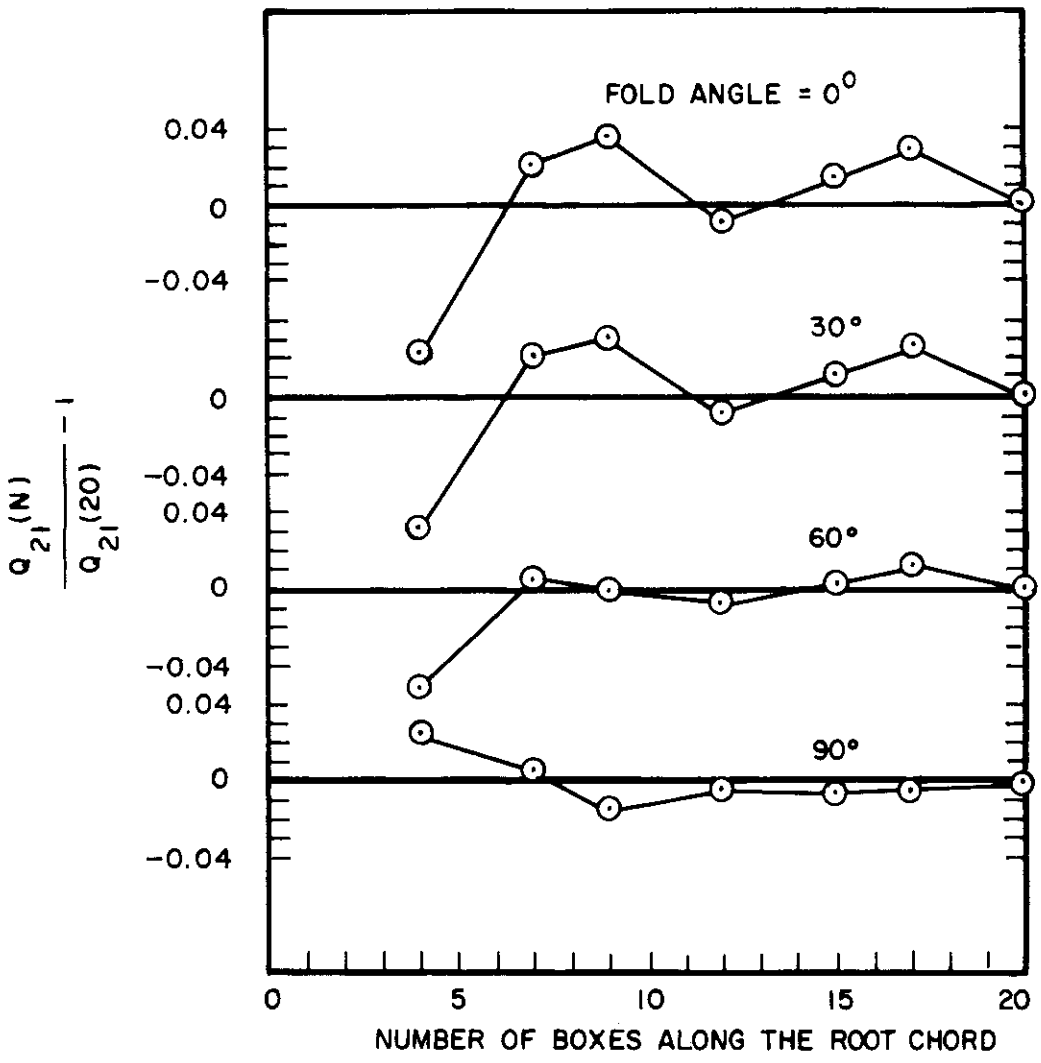

Figure 11. Variation of Oscillatory Lift Coefficient From Its Values for 20 Boxes, Cubic Camber, k = 1.0

Contrails

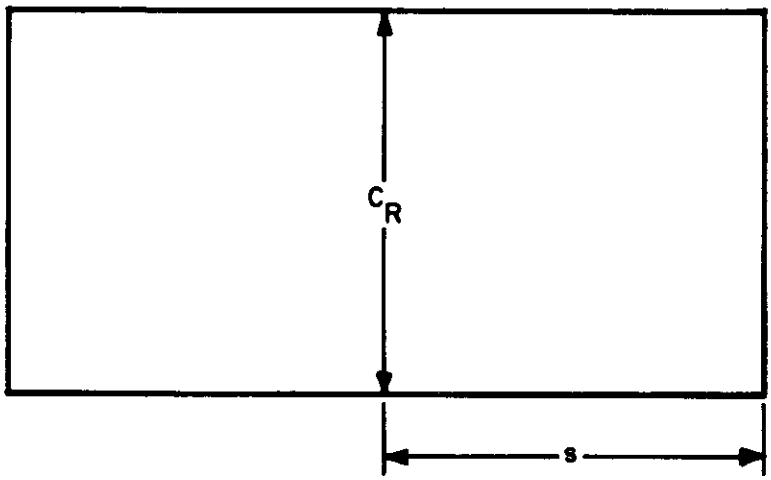

Figure 12. AGARD Aspect Ratio 2.0 Rectangular Wing, $C_R = 1.0$, s = 1.0

Contrails

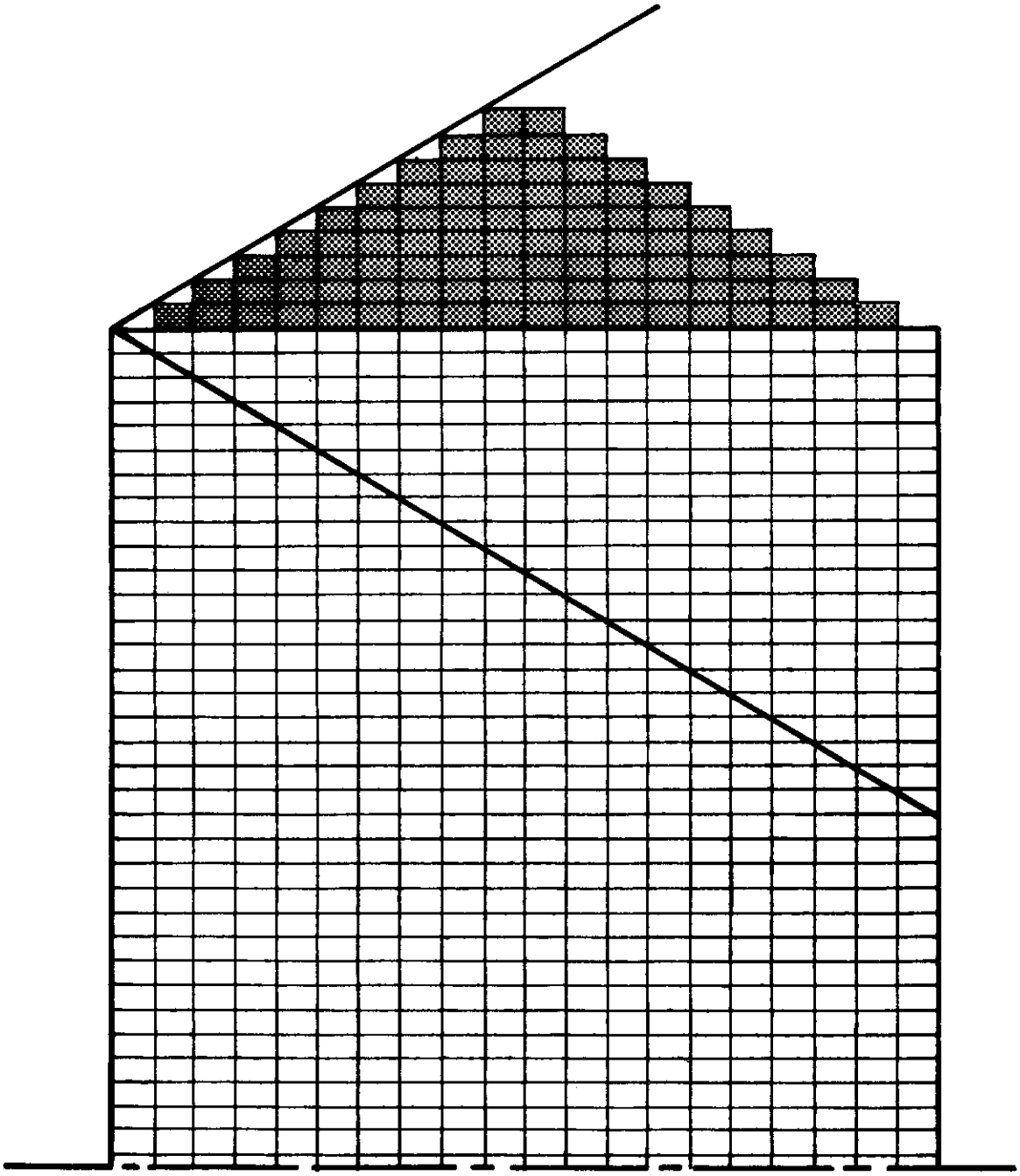

(a) $M_\infty = 2.0$

Figure 13. Mach Box Approximation to the Aspect Ratio 2.0 Rectangular Wing

Contrails

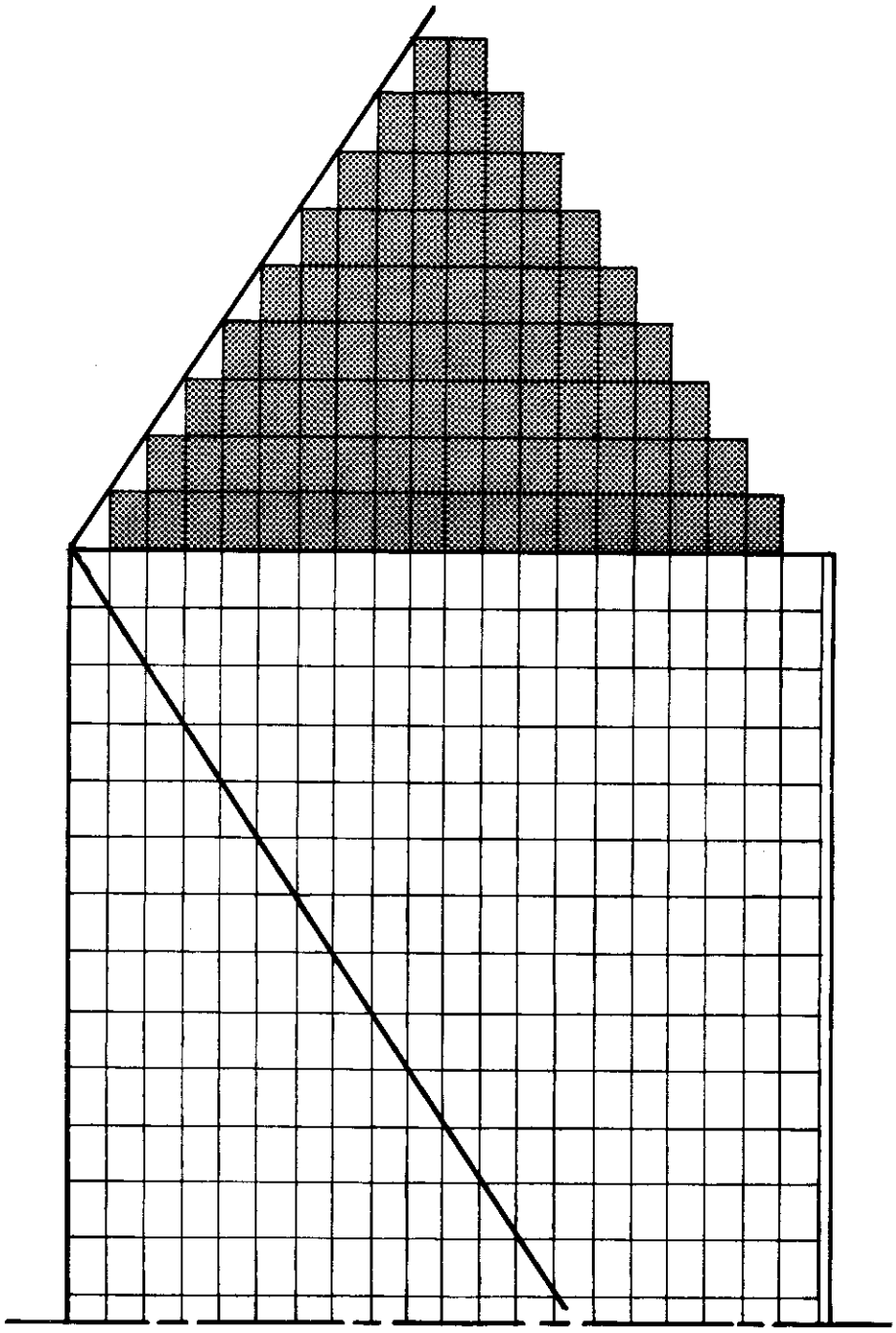

(b) $M_\infty = 1.20$

Figure 13. Mach Box Approximation to the Aspect Ratio 2.0 Rectangular Wing

Contrails

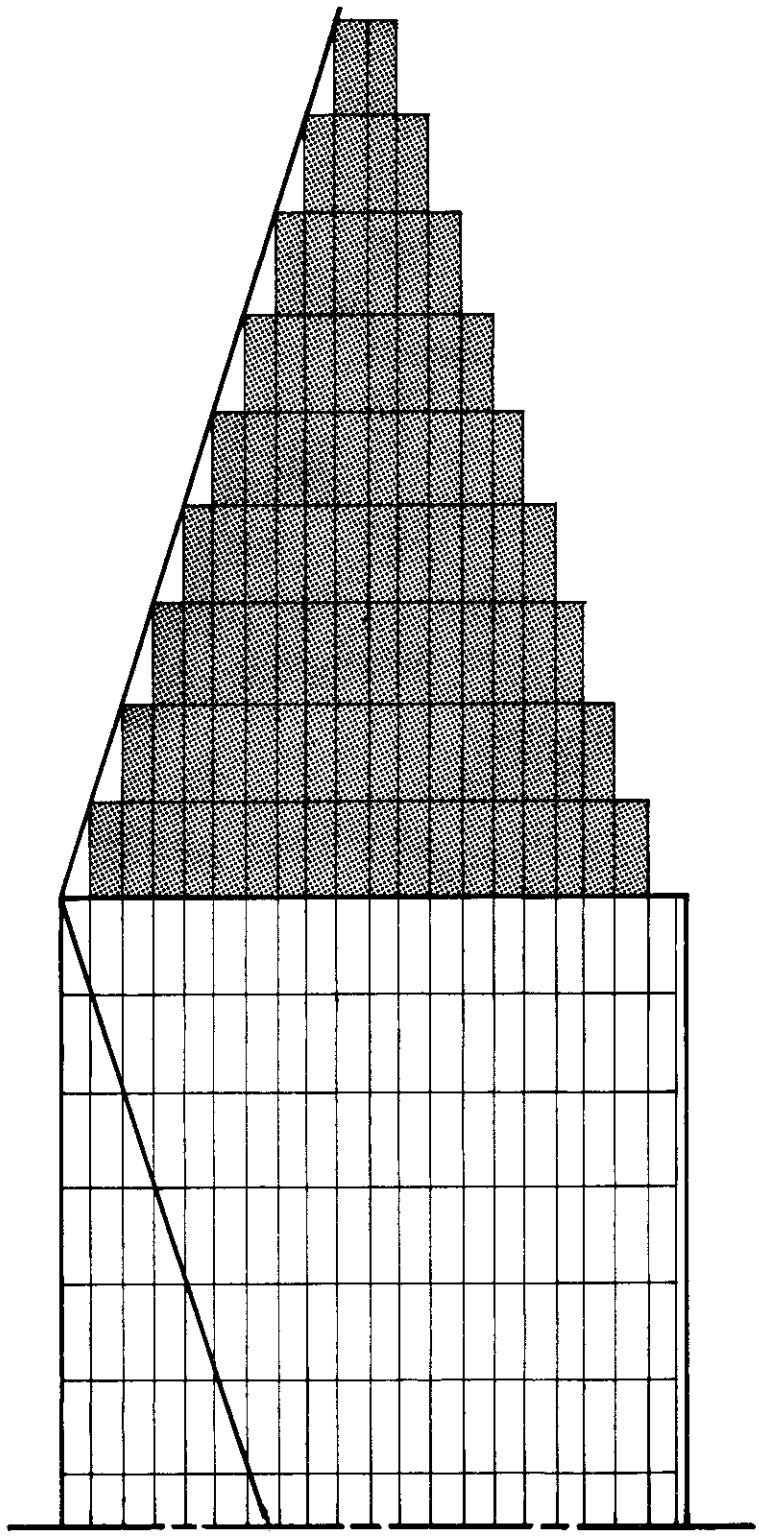

(c) $M_\infty = 1.05$

Figure 13. Mach Box Approximation to the Aspect Ratio 2.0 Rectangular Wing

Contrails

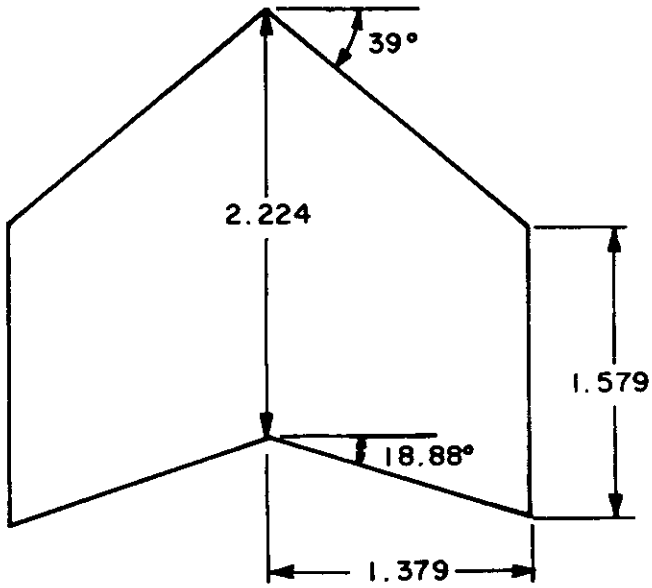

Figure 14. The AGARD Aspect Ratio 1.45 Tapered Swept-Back Wing

Contrails

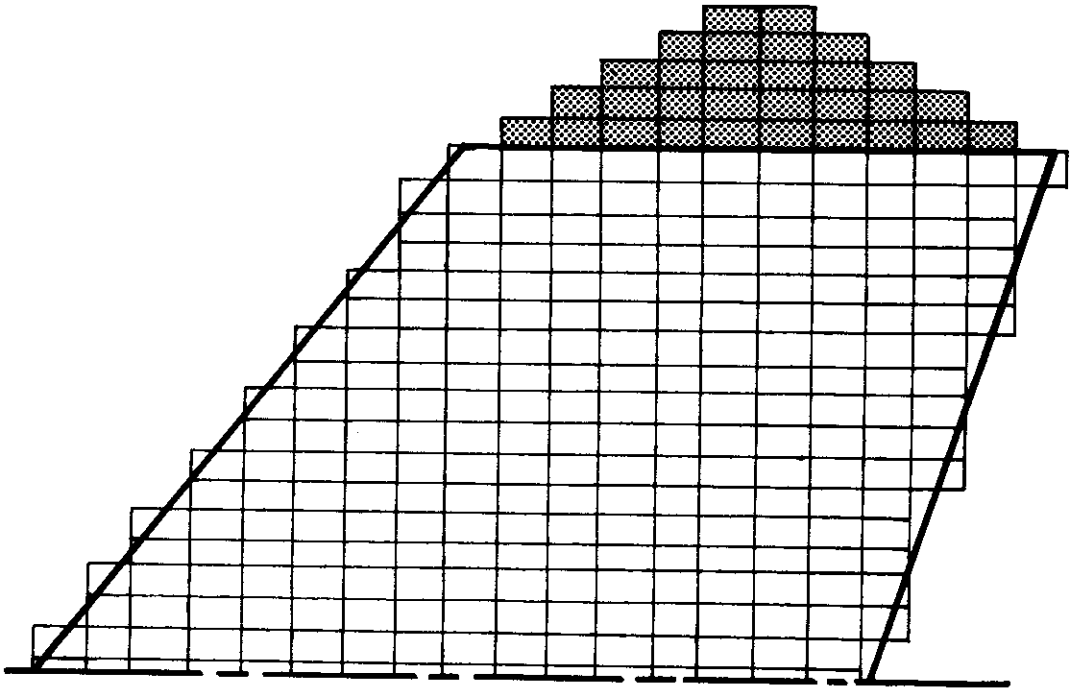

(a) $M_\infty = 2.0$

Figure 15. Mach Box Approximation to the AGARD Aspect Ratio 1.45 Tapered Swept-Back Wing

Contrails

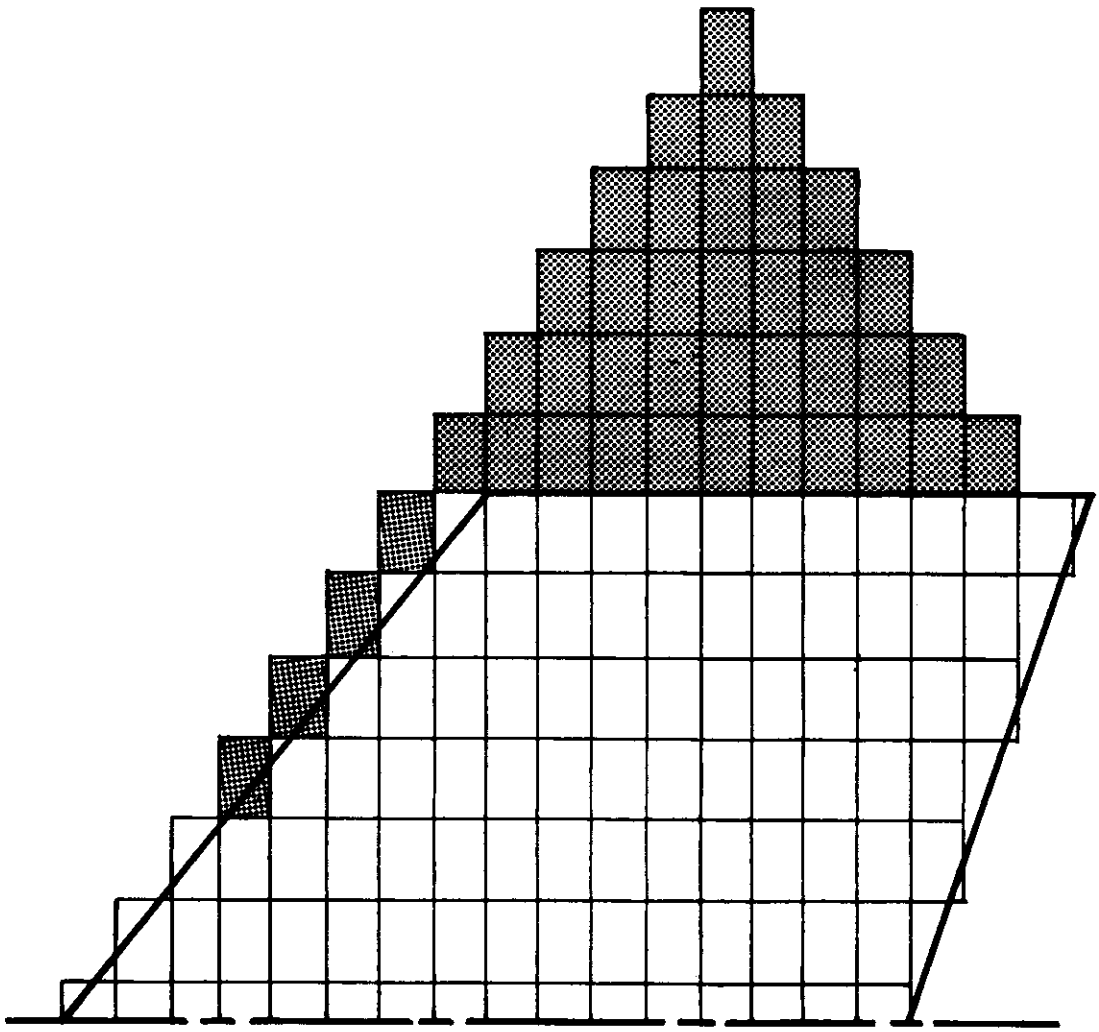

(b) $M_\infty = 1.2$

Figure 15. Mach Box Approximation to the AGARD Aspect Ratio 1.45 Tapered Swept-Back Wing

Contrails

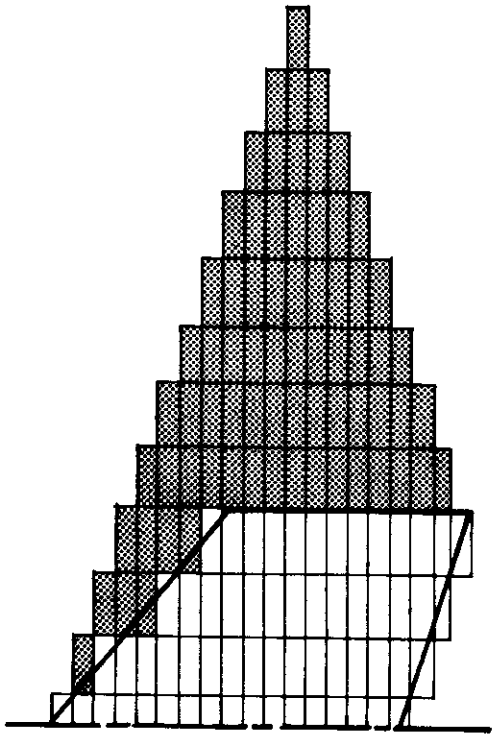

(c) $M_\infty = 1.057$

Figure 15. Mach Box Approximation to the AGARD Aspect Ratio 1.45 Tapered Swept-Back Wing

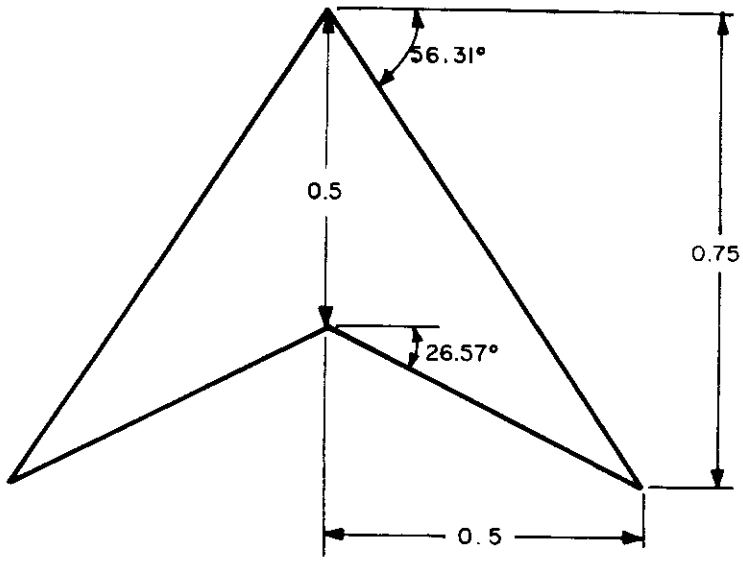

Figure 16. The AGARD Aspect Ratio 4.0 Arrowhead Wing

Contrails

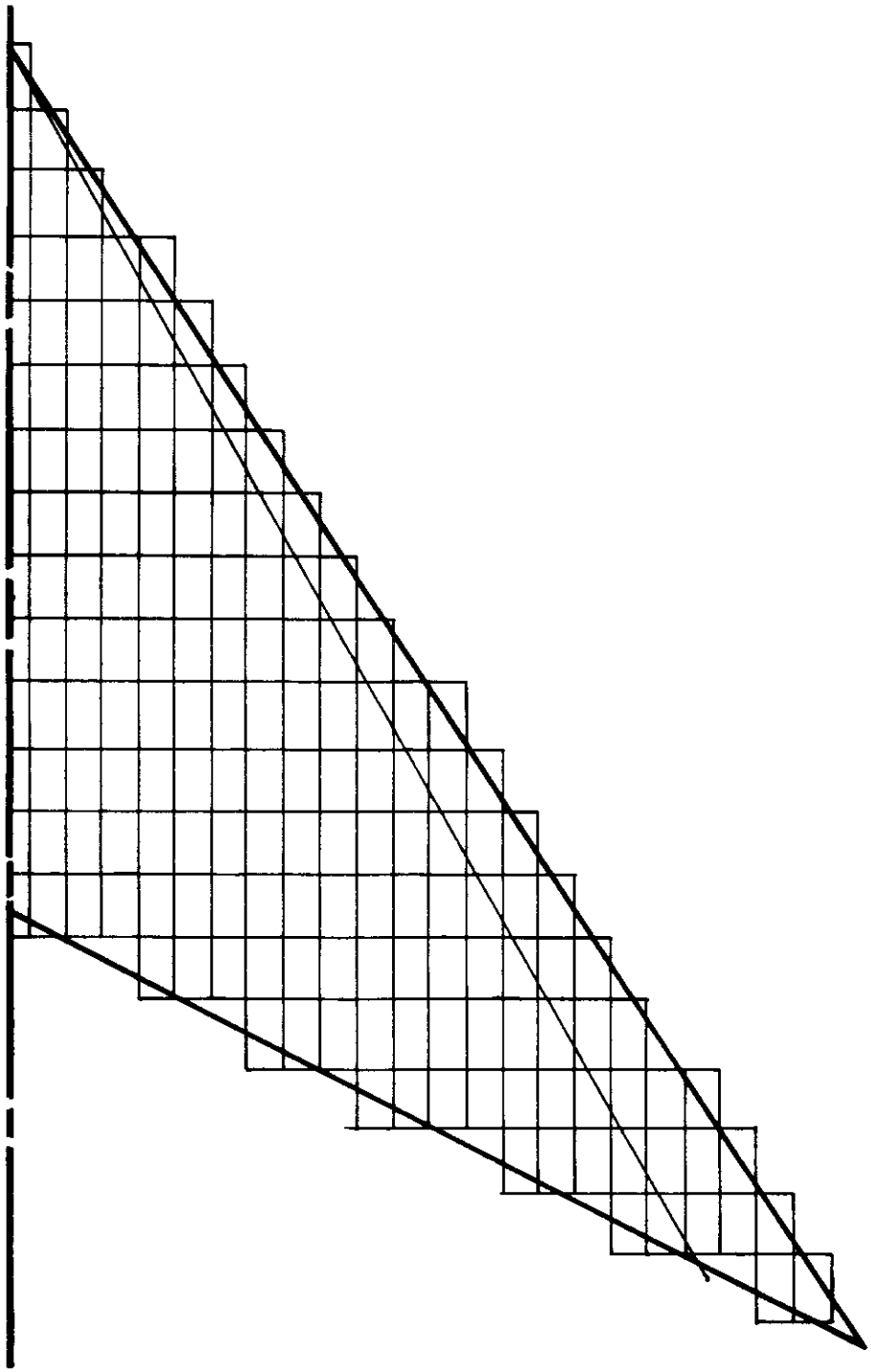

(a) $M_\infty = 2.0$

Figure 17. Mach Box Approximation to the AGARD Aspect Ratio 4.0 Arrowhead Wing

Contrails

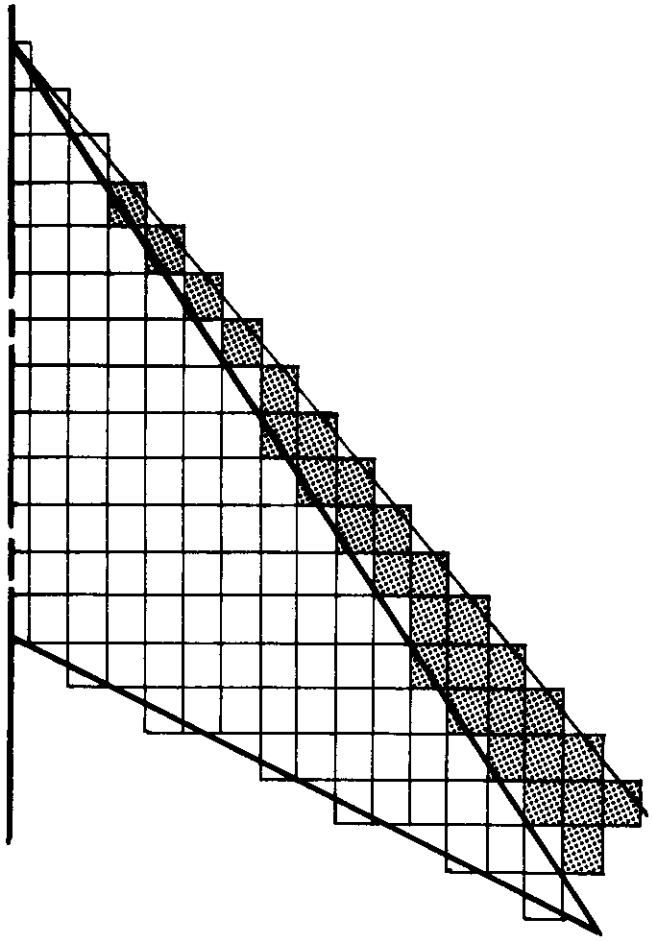

(b) $M_\infty = 1.5621$

Figure 17. Mach Box Approximation to the AGARD Aspect Ratio 4.0 Arrowhead Wing

Contrails

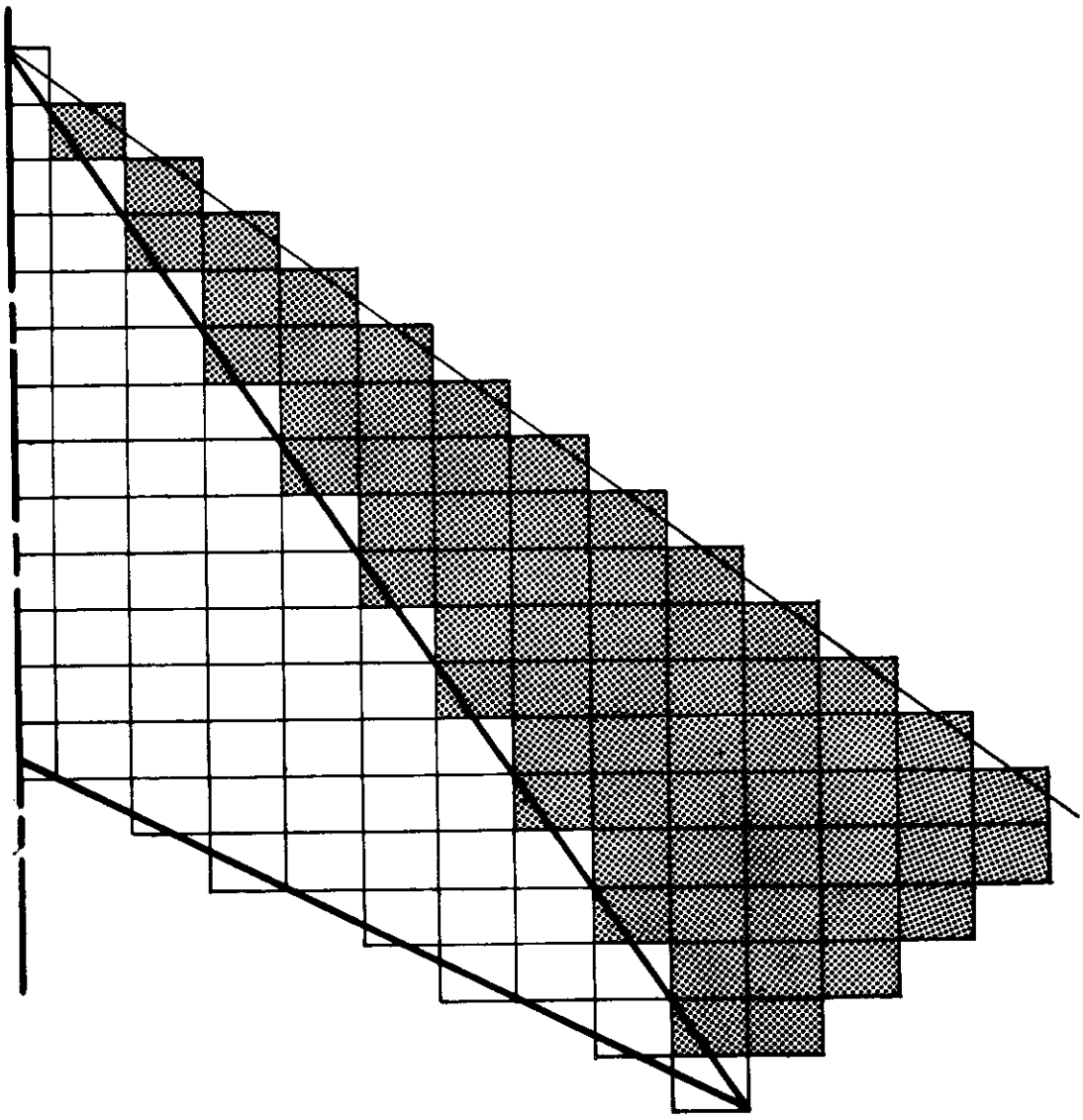

(c) $M_\infty = 1.25$

Figure 17. Mach Box Approximation to the AGARD Aspect Ratio 4.0 Arrowhead

Contrails

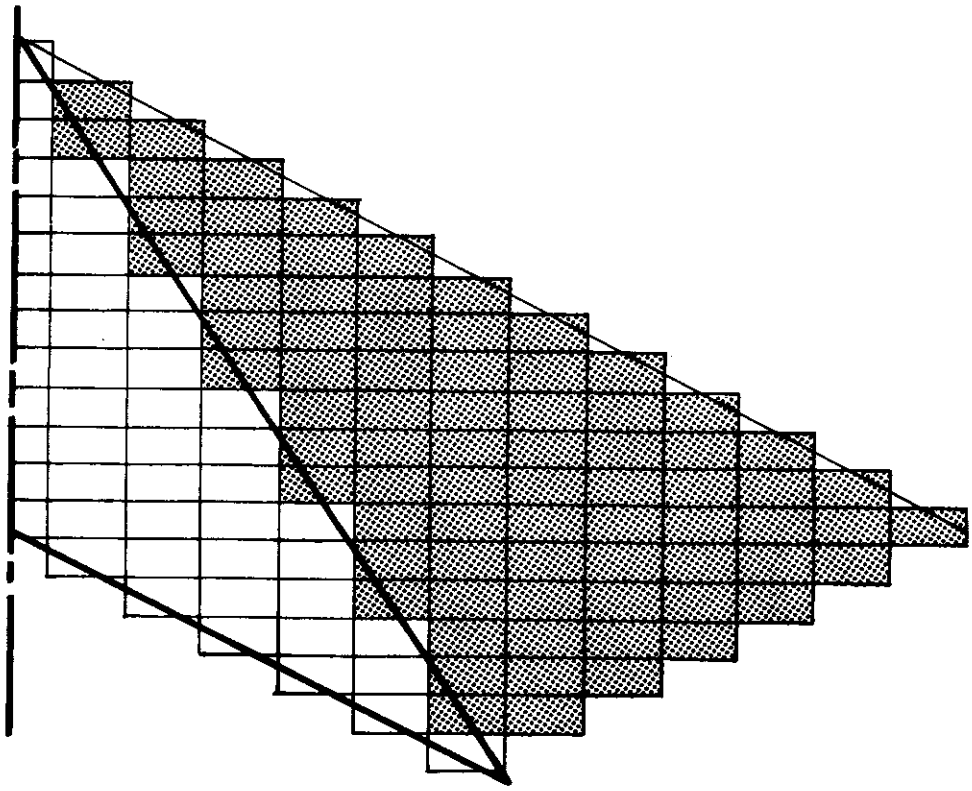

(d) $M_\infty = 1.12$

Figure 17. Mach Box Approximation to the AGARD Aspect Ratio 4.0 Arrowhead Wing

Contrails

TABLE I

INPUT DATA FOR CHECK OF MODAL INTERPRETATION

Card	Field	Entry	Explanation
1	1	2.0	Mach number
	2	12000.0	Speed of Sound
	3	30.0	Root Chord
2	1	0.0	Wing Leading Edge Sweep
	2	0.0	Wing Trailing Edge Sweep
	3	30.0	Distance, Root Chord to Fold Line
	4	0.0	Tip Leading Edge Sweep
	5	0.0	Tip Trailing Edge Sweep
	6	30.0	Distance, Root Chord to Tip Line
3	1	6	Number of Chordwise Boxes
	2	2	Number of Frequencies
	3	2	Number of Modes
	4	1	Print Velocity Potential Influence Coefficients
	5	1	Print Initial Source Strengths
	6	1	Print Final Source Strengths
4	1	1	Wing Mode is a Polynomial
	2	1	Maximum Polynomial Degree
	3	0	Irrelevant Zero
	4	1	Print Polynomial Coefficients
5	1	0	No Tip
6	1	0.0	First Frequency
	2	1.0	Number of Fold Angles
	3	2.0	Second Frequency
	4	1.0	Number of Fold Angles

Contrails

TABLE I (CONTD)

Card	Field	Entry	Explanation
7	1	0.0	Fold Angle for First Frequency
8	1	1.0	First Mode is Oscillatory
	2	10.0	Polynomial Coefficient
	3	0.0	Polynomial Coefficient
	4	0.0	Polynomial Coefficient
9	1	1.0	Second Mode is Oscillatory
	2	0.0	Polynomial Coefficient
	3	0.2	Polynomial Coefficient
	4	0.0	Polynomial Coefficient
10	1	0.0	Fold Angle for Second Frequency
11	1	1.0	First Mode is Oscillatory
	2	10.0	Polynomial Coefficient
	3	0.0	Polynomial Coefficient
	4	0.0	Polynomial Coefficient
12	1	1.0	Second Mode is Oscillatory
	2	0.0	Polynomial Coefficient
	3	0.2	Polynomial Coefficient
	4	0.0	Polynomial Coefficient
The next 12 cards are identical with the following exceptions:			
1	3	300.0	Root Chord
2	3	300.0	Distance, Root to Fold Line
	6	300.0	Distance, Root to Tip
6	3	0.2	Second Frequency

Contrails

TABLE II

OUTPUT SUMMARY FOR MODAL INTERPRETATION

$Z_1 = 10.0$ $Z_2 = 0.2X$

f (cps)	C_R	Q_{11}	Q_{12}	Q_{21}	Q_{22}
0.0	30.0	0.0	0.0	-4.03	-1.14
0.0	300.0	0.0	0.0	-4.03	-1.14x10
2.0	30.0	$-1.75\times10^{-4}-i1.05\times10^{-1}$	$-6.82\times10^{-5}-i2.99\times10^{-2}$	$-4.03-i2.69\times10^{-2}$	$-1.14-i1.07\times10^{-2}$
0.2	300.0	$-1.75\times10^{-5}-i1.05\times10^{-2}$	$-6.82\times10^{-5}-i2.99\times10^{-2}$	$-4.03-i2.69\times10^{-2}$	$-1.14\times10^{'}-i1.07\times10^{-1}$

Contrails

TABLE III

INPUT DATA FOR CONVERGENCE STUDY ON THE RECTANGULAR WING

Card	Field	Entry	Explanation
1	1	3.0	Mach Number
	2	1117.0	Speed of Sound
	3	30.0	Root Chord
2	1	0.0	Wing Leading Edge Sweep
	2	0.0	Wing Trailing Edge Sweep
	3	20.0	Distance, Root to Fold Line
	4	0.0	Tip Leading Edge Sweep
	5	0.0	Tip Trailing Edge Sweep
	6	20.0	Distance, Root to Tip
3	1	5	Chordwise Boxes
	2	1	Number of Frequencies
	3	2	Number of Modes
	4	0	Don't Print Velocity Potential Influence Coefficients
	5	0	Don't Print Initial Source Strengths
	6	1	Print Final Source Strengths
4	1	1	Wing Mode is Polynomial
	2	1	Maximum Polynomial Degree
	3	0	Irrelevant Zero
	4	1	Print Polynomial Coefficients
5	1	0	No Tip
6	1	0.0	Frequency
	2	1.0	Number of Fold Angles

Contrails

TABLE III (CONTD)

Card	Field	Entry	Explanation
7	1	0.0	Fold Angle
8	1	0.0	Don't Calculate ϕ for First Mode
	2	-5.47723	Polynomial Coefficient
	3	0.0	Polynomial Coefficient
	4	0.0	Polynomial Coefficient
9	1	1.0	Second Mode is Oscillatory
	2	0.0	Polynomial Coefficient
	3	0.182574	Polynomial Coefficient
	4	0.0	Polynomial Coefficient
These 9 cards are then repeated 9 times with the following exceptions:			
3	1	6,7,...14	Chordwise Boxes Varied
4	4	0	Don't Print Polynomials
The last case is also similar except we call for the polynomial coefficients:			
4	4	1	Print Polynomial Coefficients
All of the above cards are repeated for M = 1.5 with the exception:			
1	1	1.5	Mach Number

Contrails

TABLE IV

INPUT DATA FOR CONVERGENCE STUDY ON THE DELTA WING

Card	Field	Entry	Explanation
1	1	3.0	Mach Number
	2	1117.0	Speed of Sound
	3	30.0	Root Chord
2	1	56.31	Wing Leading Edge Sweep
	2	0.0	Wing Trailing Edge Sweep
	3	20.0	Distance, Root to Fold Line
	4	56.31	Tip Leading Edge Sweep
	5	0.0	Tip Trailing Edge Sweep
	6	20.0	Distance, Root to Tip
3	1	5	Chordwise Boxes
	2	1	Number of Frequencies
	3	2	Number of Modes
	4	0	Don't Print Velocity Potential Influence Coefficients
	5	0	Don't Print Initial Source Strengths
	6	1	Print Final Source Strengths
4	1	1	Wing Mode is Polynomial
	2	1	Maximum Polynomial Degree
	3	0	Irrelevant Zero
	4	1	Print Polynomial Coefficients
5	1	0	No Tip
6	1	0.0	Frequency
	2	1.0	Number of Fold Angles

Contrails

TABLE IV (CONTD)

Card	Field	Entry	Explanation
7	1	0.0	Fold Angle
8	1	0.0	Don't Calculate ϕ for First Mode
	2	-5.47723	Polynomial Coefficient
	3	0.0	Polynomial Coefficient
	4	0.0	Polynomial Coefficient
9	1	1.0	Second Mode is Oscillatory
	2	0.0	Polynomial Coefficient
	3	0.182574	Polynomial Coefficient
	4	0.0	Polynomial Coefficient
These 9 cards are then repeated 9 times with the following exceptions:			
3	1	6,7,...14	Chordwise Boxes Varied
4	4	0	Don't Print Polynomials
The last case is also similar except we call for the polynomial coefficients:			
4	4	1	Print Polynomial Coefficients
All of the above cards are repeated for M = 1.5 with the exception:			
1	1	1.5	Mach Number

Contrails

TABLE V

INPUT DATA FOR THE FREQUENCY CONVERGENCE STUDY

Card	Field	Entry	Explanation
1	1	1.5	Mach Number
	2	1117.0	Speed of Sound
	3	30.0	Root Chord
2	1	56.31	Wing Leading Edge Sweep
	2	0.0	Wing Trailing Edge Sweep
	3	20.0	Distance, Root chord to Fold Line
	4	56.31	Tip Leading Edge Sweep
	5	0.0	Tip Trailing Edge Sweep
	6	20.0	Distance, Root chord to Tip Line
3	1	5	Number of Boxes Along Root
	2	3	Number of Frequencies
	3	4	Number of Modes
	4	0	Don't Print Velocity Potential Influence Coefficients
	5	0	Don't Print Initial Source Strengths
	6	0	Don't Print Final Source Strengths
4	1	1	Wing Modes are Polynomials
	2	3	Maximum Polynomial Degree
	3	0	Irrelevant Zero
	4	1	Print Coefficients
5	1	0	No Tip
6	1	0.0	First Frequency
	2	1.0	Number of Fold Angles

Contrails

TABLE V (CONTD)

Card	Field	Entry	Explanation
	3	4.4445	Second Frequency
	4	1.0	Number of Fold Angles
	5	8.889	Third Frequency
	6	1.0	Number of Fold Angles
7	1	0.0	Fold Angle for First Frequency
8	1	1.0	First Mode is Oscillatory
	2	5.4772	A_1, Polynomial Coefficient
	3	0.0	A_2, Polynomial Coefficient
	4	0.0	A_3, Polynomial Coefficient
	5	0.0	A_4, Polynomial Coefficient
	6	0.0	A_5, Polynomial Coefficient
9	1	0.0	A_6, Polynomial Coefficient
	2	0.0	A_7, Polynomial Coefficient
	3	0.0	A_8, Polynomial Coefficient
	4	0.0	A_9, Polynomial Coefficient
	5	0.0	A_{10}, Polynomial Coefficient
10	1	1.0	Second Mode is Oscillatory
	2	0.0	A_1, Polynomial Coefficient
	3	0.18257	A_2, Polynomial Coefficient
	4	0.0	A_3, Polynomial Coefficient
	5	0.0	A_4, Polynomial Coefficient
	6	0.0	A_5, Polynomial Coefficient
11	1	0.0	A_6, Polynomial Coefficient
	2	0.0	A_7, Polynomial Coefficient
	3	0.0	A_8, Polynomial Coefficient

Contrails

TABLE V (CONTD)

Card	Field	Entry	Explanation
	4	0.0	A_9, Polynomial Coefficient
	5	0.0	A_{10}, Polynomial Coefficient
12	1	1.0	Third Mode is Oscillatory
	2	0.0	A_1, Polynomial Coefficient
	3	0.18257	A_2, Polynomial Coefficient
	4	0.0	A_3, Polynomial Coefficient
	5	-0.006085	A_4, Polynomial Coefficient
	6	0.0	A_5, Polynomial Coefficient
13	1	0.0	A_6, Polynomial Coefficient
	2	0.0	A_7, Polynomial Coefficient
	3	0.0	A_8, Polynomial Coefficient
	4	0.0	A_9, Polynomial Coefficient
	5	0.0	A_{10}, Polynomial Coefficient
14	1	1.0	Fourth Mode is Oscillatory
	2	0.0	A_1, Polynomial Coefficient
	3	0.18257	A_2, Polynomial Coefficient
	4	0.0	A_3, Polynomial Coefficient
	5	-0.018257	A_4, Polynomial Coefficient
	6	0.0	A_5, Polynomial Coefficient
15	1	0.0	A_6, Polynomial Coefficient
	2	0.004057	A_7, Polynomial Coefficient
	3	0.0	A_8, Polynomial Coefficient
	4	0.0	A_9, Polynomial Coefficient
	5	0.0	A_{10}, Polynomial Coefficient
Cards 7-15 are repeated twice more to yield mode shape data for the second and third frequencies. These 33 data cards must be repeated for each new value of the number of boxes.			

Contrails

TABLE VI

INPUT DATA FOR THE INTERFERENCE CONVERGENCE STUDY

Card	Field	Entry	Explanation
1	1	1.5	Mach Number
	2	1117.0	Speed of Sound
	3	30.0	Root Chord
2	1	56.31	Wing Leading Edge Sweep
	2	0.0	Wing Trailing Edge Sweep
	3	10.0	Distance, Root to Fold Line
	4	56.31	Tip Leading Edge Sweep
	5	0.0	Tip Trailing Edge Sweep
	6	20.0	Distance, Root to Tip
3	1	5	Number of Boxes
	2	1	Number of Frequencies
	3	2	Number of Modes
	4	0	Don't Print Velocity Potential Influence Coefficients
	5	0	Don't Print Initial Source Strengths
	6	1	Print Final Source Strength
4	1	1	Wing Modes are Polynomials
	2	3	Maximum Degree of Polynomials
	3	0	Irrelevant Zero
	4	1	Print Polynomial Coefficients
5	1	1	Tip Modes are Polynomials
	2	3	Maximum Degree of Polynomial
	3	0	Irrelevant Zero
	4	1	Print Polynomial Coefficients

Contrails

TABLE VI (CONTD)

Card	Field	Entry	Explanation
6	1	8.889	Frequency
	2	4.0	Number of Fold Angles
7	1	0.0	Fold Angle
8	1	0.0	Use First Wing Mode Only to Produce Generalized Forces in Mode 2.
	2	5.4772	A_1, Polynomial Coefficient in Wing First Mode
	3	0.0	A_2, Polynomial Coefficient in Wing First Mode
	4	0.0	A_3, Polynomial Coefficient in Wing First Mode
	5	0.0	A_4, Polynomial Coefficient in Wing First Mode
	6	0.0	A_5, Polynomial Coefficient in Wing First Mode
9	1	0.0	A_6, Polynomial Coefficient in Wing First Mode
	2	0.0	A_7, Polynomial Coefficient in Wing First Mode
	3	0.0	A_8, Polynomial Coefficient in Wing First Mode
	4	0.0	A_9, Polynomial Coefficient in Wing First Mode
	5	0.0	A_{10}, Polynomial Coefficient in Wing First Mode
10	1	1.0	Second Wing Mode is Oscillatory Type
	2	0.0	A_1, Polynomial Coefficient in Wing Second Mode
	3	0.18257	A_2, Polynomial Coefficient in Wing Second Mode
	4	0.0	A_3, Polynomial Coefficient in Wing Second Mode

Contrails

TABLE VI (CONTD)

Card	Field	Entry	Explanation
	5	-0.018257	A_4, Polynomial Coefficient in Wing Second Mode
	6	0.0	A_5, Polynomial Coefficient in Wing Second Mode
11	1	0.0	A_6, Polynomial Coefficient in Wing Second Mode
	2	0.004057	A_7, Polynomial Coefficient in Wing Second Mode
	3	0.0	A_8, Polynomial Coefficient in Wing Second Mode
	4	0.0	A_9, Polynomial Coefficient in Wing Second Mode
	5	0.0	A_{10}, Polynomial Coefficient in Wing Second Mode
12	1	0.0	Use First Tip Mode Only to Produce Generalized Forces in Mode 2
	2	5.4772	A_1, Polynomial Coefficient in Tip First Mode
	3	0.0	A_2, Polynomial Coefficient in Tip First Mode
	4	0.0	A_3, Polynomial Coefficient in Tip First Mode
	5	0.0	A_4, Polynomial Coefficient in Tip First Mode
	6	0.0	A_5, Polynomial Coefficient in Tip First Mode
13	1	0.0	A_6, Polynomial Coefficient in Tip First Mode
	2	0.0	A_7, Polynomial Coefficient in Tip First Mode
	3	0.0	A_8, Polynomial Coefficient in Tip First Mode
	4	0.0	A_9, Polynomial Coefficient in Tip First Mode

Contrails

TABLE VI (CONTD)

Card	Field	Entry	Explanation
	5	0.0	A_{10}, Polynomial Coefficient in Tip First Mode
14	1	1.0	Second Tip Mode is Oscillatory Type
	2	0.0	A_1, Polynomial Coefficient in Tip Second Mode
	3	0.18257	A_2, Polynomial Coefficient in Tip Second Mode
	4	0.0	A_3, Polynomial Coefficient in Tip Second Mode
	5	-0.018257	A_4, Polynomial Coefficient in Tip Second Mode
	6	0.0	A_5, Polynomial Coefficient in Tip Second Mode
15	1	0.0	A_6, Polynomial Coefficient in Tip Second Mode
	2	0.004057	A_7, Polynomial Coefficient in Tip Second Mode
	3	0.0	A_8, Polynomial Coefficient in Tip Second Mode
	4	0.0	A_9, Polynomial Coefficient in Tip Second Mode
	5	0.0	A_{10}, Polynomial Coefficient in Tip Second Mode

Cards 7-15 are repeated three times for fold angles of 30 degrees, 60 degrees and 90 degrees for a total of 42 cards. The polynomial coefficients of the tip modes are multiplied by the cosine of the fold angle.

The entire deck of 42 cards must be repeated for each new number of boxes used along the chord.

Contrails

TABLE VII

MACH NUMBER, k_s, AND FREQUENCY FOR THE AGARD ASPECT RATIO 2.0 RECTANGLE

M	k_s	f (cps)
1.05	0	0
	0.3	50.14
	0.6	100.3
	1.0	167.1
	2.0	334.2
1.20	0	0
	0.3	57.30
	0.6	114.6
	1.0	191.0
	2.0	382.0
2.00	0	0
	0.3	95.51
	0.6	191.0
	1.0	318.4
	2.0	636.6

Contrails

TABLE VIII

MODE SHAPES FOR THE ASPECT RATIO 2.0 RECTANGULAR WING
IN AGARD AND MACH BOX COORDINATE SYSTEMS

Mode	f (x,y)	Z (X,Y)
1	1	1
2	x	-0.5 + X
3	x^2	$0.25 - X + X^2$
4	y^2	Y^2
5	x^2y^2	$0.25Y^2 - XY^2 + X^2Y^2$
6	$\|y\|$	$\|Y\|$
7	$x\|y\|$	$-0.5\|Y\| + X\|Y\|$

Contrails

TABLE IX

$Q_{ij}^{\cdot}$ IN AGARD NOTATION, ASPECT RATIO 2.0 RECTANGLE

(a) $M_\infty = 2.0$, $k_S = 0.0$

I	J=1	J=2	J=3	J=4	J=5	J=6	J=7
1	0.0	1.988,0	1.123,-1	0.0	7.554,-2	0.0	8.478,-1
2	0.0	-5.579,-2	3,864,-1	0.0	1.235,-1	0.0	-5.105,-2
3	0.0	1.660,-1	5.713,-3	0.0	2.792,-3	0.0	7.142,-2
4	0.0	4.631,-2	2.165,-1	0.0	1.199,-1	0.0	3.709,-2
5	0.0	-7.542,-2	3.870,-2	0.0	1.521,-2	0.0	-4.369,-2
6	0.0	-1.704,-1	4.184,-1	0.0	1.621,-1	0.0	8.621,-3
7	0.0	4.809,-1	2.424,-2	0.0	4.818,-2	0.0	1.914,-1

(b) $M_\infty = 1.20$, $k_S = 0.0$

I	J=1	J=2	J=3	J=4	J=5	J=6	J=7
1	0.0,-0	3.836,-0	7.603,-1	0.0,-0	3.439,-1	0.0,-0	1.180,-0
2	0.0,-0	-3.783,-1	1.021,-0	0.0,-0	2.800,-1	0.0,-0	-2.559,-1
3	0.0,-0	3.264,-1	4.290,-2	0.0,-0	7.144,-3	0.0,-0	1.202,-1
4	0.0,-0	-3.603,-2	4.916,-1	0.0,-0	2.200,-1	0.0,-0	-7.159,-2
5	0.0,-0	-1.552,-1	6.702,-2	0.0,-0	9.345,-3	0.0,-0	-6.860,-2
6	0.0,-0	-6.793,-1	1.005,-0	0.0,-0	3.368,-1	0.0,-0	-2.380,-1
7	0.0,-0	9.670,-1	1.201,-1	0.0,-0	1.120,-1	0.0,-0	2.591,-1

(c) $M_\infty = 1.05$, $k_S = 0.0$

I	J=1	J=2	J=3	J=4	J=5	J=6	J=7
1	0.000,0	3.776,0	2.693,0	0.000,0	6,095,-1	0.000,0	1.008,0
2	0.000,0	-1.348,0	1.921,0	0.000,0	3.527,-1	0.000,0	-4.343,-1
3	0.000,0	3.770,-1	8.046,-2	0.000,0	-1.440,-2	0.000,0	1.782,-1
4	0.000,0	-4.093,-1	9.456,-1	0.000,0	2.687,-1	0.000,0	-1.640,-1
5	0.000,0	-2.442,-1	7.697,-2	0.000,0	-5.394,-3	0.000,0	-6.413,-2
6	0.000,0	-1.604,0	1.737,0	0.000,0	3.967,-1	0.000,0	-4.060,-1
7	0.000,0	1.036,0	5.357,-1	0.000,0	1.742,-1	0.000,0	2.113,-1

Contrails

TABLE X

MACH NUMBER, k_s, AND FREQUENCY FOR THE AGARD ASPECT RATIO 1.45 TAPERED, SWEPT-BACK WING

M	k_s	f (cps)
2.0	0.0	0.0
	0.5	115.4
	1.4	323.2
1.2	0.0	0.0
	0.5	69.3
	1.4	193.9
1.057	0.0	0.0
	0.5	61.0
	1.4	171.0

Contrails

TABLE XI

MODE SHAPES FOR THE ASPECT RATIO 1.45 TAPERED, SWEPT-BACK WING IN AGARD AND MACH BOX COORDINATE SYSTEMS

Mode	f (x,y)	Z (X,Y)
1	1.0	1.379
2	x	-1.112 + X
3	x^2	$0.8967 - 1.613X + .7252X^2$
4	y^2	$0.7252Y^2$
5	$\|y\|$	$\|Y\|$
6	$x\|y\|$	$-0.8064\|Y\| + 0.7252X\|Y\|$

Contrails

TABLE XII

Q'_{ij} IN AGARD NOTATION, ASPECT RATIO 1.45 TAPERED, SWEPT- BACK WING

(a) $M_\infty = 2.0$, $k_S = 0.0$

I	J=1	J=2	J=3	J=4	J=5	J=6
1	0.000,0	2.667,0	1.527,0	0.000,0	0.000,0	9.742,-1
2	0.000,0	4.866,-1	1.533,0	0.000,0	0.000,0	1.988,-1
3	0.000,0	5.629,-1	8.727,-1	0.000,0	0.000,0	1.722,-1
4	0.000,0	-1.875,-1	4.201,-1	0.000,0	0.000,0	-8.662,-2
5	0.000,0	-8.714,-1	8.355,-1	0.000,0	0.000,0	-2.251,-1
6	0.000,0	1.974,0	6.996,-1	0.000,0	0.000,0	7.383,-1

(b) $M_\infty = 1.2$, $k_S = 0.0$

I	J=1	J=2	J=3	J=4	J=5	J=6
1	0.000,0	4.185,0	4.265,0	0.000,0	0.000,0	1.061,0
2	0.000,0	4.800,-2	3.574,0	0.000,0	0.000,0	-1.748,-1
3	0.000,0	6.378,-1	1.911,0	0.000,0	0.000,0	1.222,-2
4	0.000,0	-6.576,-1	8.724,-1	0.000,0	0.000,0	-3.018,-1
5	0.000,0	-2.144,0	1.492,0	0.000,0	0.000,0	-6.584,-1
6	0.000,0	3.258,0	2.128,0	0.000,0	0.000,0	8.911,-1

(c) $M_\infty = 1.057$, $k_S = 0.0$

I	J=1	J=2	J=3	J=4	J=5	J=6
1	0.000,0	3.680,0	6.419,0	0.000,0	0.000,0	8.929,-1
2	0.000,0	-9.459,-1	4.301,0	0.000,0	0.000,0	-3.309,-1
3	0.000,0	1.144,-1	2.178,0	0.000,0	0.000,0	2.817,-2
4	0.000,0	-9.734,-1	8.306,-1	0.000,0	0.000,0	-3.234,-1
5	0.000,0	-2.882,0	1.102,0	0.000,0	0.000,0	-7.118,-1
6	0.000,0	3.242,0	3.523,0	0.000,0	0.000,0	8.480,-1

Contrails

TABLE XIII

MACH NUMBER, k_s, AND FREQUENCY FOR THE AGARD ASPECT RATIO 4.0 ARROWHEAD WING

M	k_s	f (cps)
2.0	0.0	0.0
	0.5	318.3
	1.0	636.6
	2.0	1273.3
	4.0	2546.6
1.5621	0.0	0.0
	0.5	248.6
	1.0	497.2
	2.0	994.5
	4.0	1989.0
1.25	0.0	0.0
	0.5	198.9
	1.0	397.9
	2.0	795.8
	4.0	1591.6
1.12	0.0	0.0
	0.5	178.3
	1.0	356.5
	2.0	713.0
	4.0	1426.1

Contrails

TABLE XIV

MODE SHAPES FOR THE ASPECT RATIO 4.0 ARROWHEAD WING
IN AGARD AND MACH BOX COORDINATE SYSTEMS

Mode	f (x,y)	Z (X,Y)
1	1	0.5
2	x	-0.25 + X
3	x^2	0.125 - X + 2.0 X^2
4	y^2	2.0 Y^2
5	$\|y\|$	$\|Y\|$
6	$x\|y\|$	-0.5$\|Y\|$ + 2.0 $X\|Y\|$

Contrails

TABLE XV

Q'_{ij} IN AGARD NOTATION, ASPECT RATIO 4.0 ARROWHEAD WING

(a) $M_\infty = 2.0$, $k_S = 0.0$

I	J=1	J=2	J=3	J=4	J=5	J=6
1	0.000,0	1.264,0	8.020,-1	0.000,0	0.000,0	4.063,-1
2	0.000,0	4.643,-1	5.162,-1	0.000,0	0.000,0	2.096,-1
3	0.000,0	3.164,-1	3.114,-1	0.000,0	0.000,0	1.472,-1
4	0.000,0	1.608,-1	2.073,-1	0.000,0	0.000,0	9.877,-2
5	0.000,0	9.266,-2	3.190,-1	0.000,0	0.000,0	1.176,-1
6	0.000,0	4.879,-1	3.259,-1	0.000,0	0.000,0	1.897,-1

(b) $M_\infty = 1.5621$, $k_S = 0.0$

I	J=1	J=2	J=3	J=4	J=5	J=6
1	0.000,0	1.584,0	1.099,0	0.000,0	0.000,0	4.837,-1
2	0.000,0	5.459,-1	6.555,-1	0.000,0	0.000,0	2.322,-1
3	0.000,0	3.506,-1	3.822,-1	0.000,0	0.000,0	1.478,-1
4	0.000,0	1.868,-1	2.412,-1	0.000,0	0.000,0	1.035,-1
5	0.000,0	8.154,-2	3.706,-1	0.000,0	0.000,0	1.176,-1
6	0.000,0	6.134,-1	4.215,-1	0.000,0	0.000,0	2.168,-1

(c) $M_\infty = 1.25$, $k_S = 0.0$

I	J=1	J=2	J=3	J=4	J=5	J=6
1	0.000,0	1.940,0	1.834,0	0.000,0	0.000,0	6.308,-1
2	0.000,0	7.290,-1	1.075,0	0.000,0	0.000,0	3.233,-1
3	0.000,0	4.940,-1	6.762,-1	0.000,0	0.000,0	2.187,-1
4	0.000,0	3.041,-1	4.514,-1	0.000,0	0.000,0	1.621,-1
5	0.000,0	1.901,-1	6.180,-1	0.000,0	0.000,0	1.808,-1
6	0.000,0	8.072,-1	7.631,-1	0.000,0	0.000,0	3.001,-1

(d) $M_\infty = 1.12$, $k_S = 0.0$

I	J=1	J=2	J=3	J=4	J=5	J=6
1	0.000,0	2.353,0	2.539,0	0.000,0	0.000,0	8.202,-1
2	0.000,0	9.641,-1	1.497,0	0.000,0	0.000,0	4.455,-1
3	0.000,0	6.800,-1	9.726,-1	0.000,0	0.000,0	3.121,-1
4	0.000,0	4.225,-1	6.663,-1	0.000,0	0.000,0	2.269,-1
5	0.000,0	3.217,-1	8.810,-1	0.000,0	0.000,0	2.612,-1
6	0.000,0	9.949,-1	1.099,0	0.000,0	0.000,0	3.929,-1

Contrails

Contrails

APPENDIX

INTERPRETATION OF MODE SHAPES

Introduce a right-hand coordinate system X, Y, Z; $\tilde{\xi}, \tilde{\eta}, \tilde{\zeta}$, where each coordinate has the physical dimensions of length

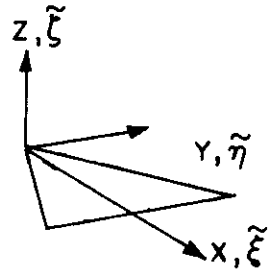

The amplitude of the oscillatory deflection of the surface at X, Y, is given by Z (X,Y), and the downwash at that point is given by

$$W(X,Y) = -\left[U \frac{dZ(X,Y)}{dX} + i\omega Z(X,Y)\right]$$

Hence the nondimensional downwash or "local angle of attack" is given by

$$\alpha(X,Y) = \frac{W(X,Y)}{U} = -\left[\frac{dZ(X,Y)}{dX} + i \frac{kZ(X,Y)}{C_R}\right]$$

where C_R is some typical dimension, say the root chord, and k is the "reduced" frequency $C_R \omega/U$.

At this point we define a generalized force coefficient Q_{ij} as was done in Reference 1 by:

$$Q_{ij} = \frac{1}{qS} \iint_S Z_i(X,Y)\, \Delta P_j(X,Y)\, dX\, dY$$

where S is the wing area, Z_i is the deflection in the i^{th} mode and ΔP_j is the pressure difference across the surface in the J^{th} mode (positive in the direction of positive Z).

When first using a computer program we are not sure whether X, Y, Z have been nondimensionalized. Hence we assume the deflection is given by a fairly general polynomial form:

$$\frac{Z(X,Y)}{C_R^r} = \sum_{ij} A_{ij} \left(\frac{X}{C_R^t}\right)^i \left(\frac{Y}{C_R^t}\right)^j$$

Contrails

For instance a plunge mode would be given by

$$Z\,(X,Y) = A_{\infty}\ C_R^r$$

and a rotation about the leading edge would be given by

$$Z\,(X,Y) = A_{10}\ X\ C_R^{r-t}$$

Our purpose is to determine what values to assign to the powers r and t. We can note that the pressure differential at X, Y can be given by

$$\Delta P_j\,(X,Y) = \iint_S \frac{\partial \Delta P}{\partial \alpha}(X,Y;\tilde{\xi},\tilde{\eta})\,\alpha_j(\tilde{\xi},\tilde{\eta})\,d\tilde{\xi}\,d\tilde{\eta}$$

Then the generalized force coefficient becomes

$$Q_{ij} = \frac{1}{qS}\iint_S Z_i\,(X,Y)\left[\iint_S \frac{\partial \Delta P}{\partial \alpha}(X,Y;\tilde{\xi},\tilde{\eta})\,\alpha_j\,(\tilde{\xi},\tilde{\eta})\,d\tilde{\xi}\,d\tilde{\eta}\right] dX\,dY$$

Dropping the A_{ij} notation in favor of a simpler one, we define the first mode by $Z_1 = A_1 C_R^r$ and the second mode by $Z_2 = A_2 X C_R^{r-t}$

If we introduce abbreviations for the following integrals in analogy with the steady-state case:

$$C_{L_\alpha} = \frac{1}{qS}\iint_S\left[\iint_S \frac{\partial \Delta P}{\partial \alpha}\,(X,Y;\tilde{\xi},\tilde{\eta})\,d\tilde{\xi}\,d\tilde{\eta}\right] dX\,dY$$

$$C_R C_{M_\alpha} = \frac{1}{qS}\iint_S X\left[\iint_S \frac{\partial \Delta P}{\partial \alpha}\,(X,Y;\tilde{\xi},\tilde{\eta})\,d\tilde{\xi}\,d\tilde{\eta}\right] dX\,dY$$

$$C_R^2 C_{F_\alpha} = \frac{1}{qS}\iint_S X^2\left[\iint_S \frac{\partial \Delta P}{\partial \alpha}\,(X,Y;\tilde{\xi},\tilde{\eta})\,d\tilde{\xi}\,d\tilde{\eta}\right] dX\,dY$$

Contrails

The generalized force coefficients* become

$$Q_{11} = -ik\, A_1^2\, C_R^{2r-1}\, C_{L_\alpha}$$

$$Q_{12} = -A_1 A_2 C_R^{2r-t}\, (C_{L_\alpha} + i\, k\, C_{M_\alpha})$$

$$Q_{21} = -ik\, A_1 A_2 C_R^{2r-t}\, C_{M_\alpha}$$

$$Q_{22} = -A_2^2\, C_R^{2r-2t+1}\, (C_{M_\alpha} + ik\, C_{F_\alpha})$$

Now suppose that we make computer runs on two geometrically similar wings at the same k and with the same coefficients A_1 and A_2, but with different root chords. Since C_{L_α}, C_{M_α}, and C_{F_α} will remain constant between the two runs, the ratios of the root chords and generalized forces between the two runs are

$$R_{11} = R_c^{2r-1}$$

$$R_{12} = R_c^{2r-t}$$

$$R_{21} = R_c^{2r-t}$$

$$R_{22} = R_c^{2r-2t+1}$$

*It is important to note that if the generalized force coefficient Q_{ij} is defined in the transpose sense:

$$Q_{ij} = \frac{1}{qS} \iint_S \Delta P_i\,(X,Y)\, Z_j\,(X,Y)\, dX\, dY$$

then all of the subscripts given above must be transposed. As shown in Section I, this latter definition is in fact the one used in the computer program, and the former definition is the one used in Reference 1.

Contrails

Here we have four equations for the two unknowns r and t. Various combinations of the above equations yield the following solutions, all of which should be consistent.

$$r = \frac{1}{2}(1 + \log R_{11}/\log R_c)$$

$$r = \frac{1}{2}(1 - \log R_{22}/\log R_c)$$

$$t = 1 - \log (R_{22}/R_{12})/\log R_c$$

$$t = 1 - \log (R_{22}/R_{21})/\log R_c$$

$$t = 1 + \log (R_{11}/R_{21})/\log R_c$$

$$t = 1 + \log (R_{11}/R_{12})/\log R_c$$

$$t = 1 + \frac{\log (R_{11}/R_{22})}{2 \log R_c}$$

These equations for r and t are the same whether we use

$$Q_{ij} = \frac{1}{qS} \iint_S \Delta P_i (X,Y)\, Z_j (X,Y)\, dX\, dY$$

or

$$Q_{ij} = \frac{1}{qS} \iint_S \Delta P_j (X,Y)\, Z_i (X,Y)\, dX\, dY$$

Contrails

UNCLASSIFIED

Security Classification

DOCUMENT CONTROL DATA - R & D

(Security classification of title, body of abstract and indexing annotation must be entered when the overall report is classified)

1. ORIGINATING ACTIVITY *(Corporate author)*
Air Force Flight Dynamics Laboratory (FDDS)
Wright-Patterson Air Force Base, Ohio 45433

2a. REPORT SECURITY CLASSIFICATION
UNCLASSIFIED

2b. GROUP

3. REPORT TITLE
DEMONSTRATION OF A SUPERSONIC BOX METHOD FOR UNSTEADY AERODYNAMICS OF NONPLANAR WINGS - Part I. General Applications

4. DESCRIPTIVE NOTES *(Type of report and inclusive dates)*
March 1967 - September 1968

5. AUTHOR(S) *(First name, middle initial, last name)*
Olsen, James J.

6. REPORT DATE	7a. TOTAL NO. OF PAGES	7b. NO. OF REFS
February 1969	77	5

8a. CONTRACT OR GRANT NO.

b. PROJECT NO. 1370

c. Task 137003

d.

9a. ORIGINATOR'S REPORT NUMBER(S)
AFFDL-TR-67-104
Part I

9b. OTHER REPORT NO(S) *(Any other numbers that may be assigned this report)*

10. DISTRIBUTION STATEMENT
This document is subject to special export controls and each transmittal to foreign governments or foreign nationals may be made only with prior approval of the Vehicle Dynamics Division (FDD), Air Force Flight Dynamics Laboratory, Wright-Patterson AFB, Ohio.

11. SUPPLEMENTARY NOTES
None

12. SPONSORING MILITARY ACTIVITY
Air Force Flight Dynamics Laboratory (FDDS)
Wright-Patterson Air Force Base, Ohio 45433

13. ABSTRACT

This report is published in two parts: Part I, "General Application," and Part II, "Application to the AGARD Planforms."

Part I presents and interprets the calculations of the unsteady aerodynamic prediction method known as the "Nonplanar Mach Box" method. It contains examples of data input and output for the associated computer program and explains the program's interpretation of the user's modal data. Also included are summaries of convergence properties, comparison with exact linearized theory, and a brief outline of the calculations for the Advisory Group for Aeronautical Research and Development (AGARD) planforms. A small part of the extensive tables of Part II is included in Part I.

Part II contains a tabulation of the "Nonplanar Mach Box" results for unsteady generalized force coefficients for the planforms, Mach numbers, mode shapes, and frequencies recommended by AGARD. The tabulation used the AGARD coordinate system and format. Not all the desired cases could be included because of the program's current limitation to supersonic trailing edges (leading edges can be supersonic or subsonic).

The method was found to be fully workable and constitutes a valuable research and design tool. Convergence and accuracy were found to be comparable to steady-state, planar methods. The computer program is available with sample problems from the Air Force Flight Dynamics Laboratory.

DD FORM 1 NOV 65 1473

UNCLASSIFIED

Security Classification

Contrails

14. KEY WORDS	LINK A		LINK B		LINK C	
	ROLE	WT	ROLE	WT	ROLE	WT
Unsteady Aerodynamics						
Supersonic Mach Box						
Interference						
AGARD Planforms						